DAMBRK: THE NWS DAM-BREAK FLOOD FORECASTING MODEL

D. L. Fread

Office of Hydrology, National Weather Service (NWS)
Silver Spring, Maryland 20910

July 18, 1984

1. INTRODUCTION

Catastrophic flash flooding occurs when a dam is breached and the impounded water escapes through the breach into the downstream valley. Usually the response time available for warning is much shorter than for precipitation-runoff floods. Dam failures are often caused by overtopping of the dam due to inadequate spillway capacity during large inflows to the reservoir from heavy precipitation runoff. Dam failures may also be caused by seepage or piping through the dam or along internal conduits, slope embankment slides, earthquake damage and liquefaction of earthen dams from earthquakes, and landslide-generated waves within the reservoir. Middlebrooks (1952) describes earthen dam failures occurring within the U.S. prior to 1951. Johnson and Illes (1976) summarize 300 dam failures throughout the world.

The potential for catastrophic flooding due to dam failures has recently been brought to the Nation's attention by several dam failures such as the Buffalo Creek coal-waste dam, the Toccoa Dam, the Teton Dam, and the Laurel Run Dam. A report by the U.S. Army (1975) gives an inventory of the Nation's approximately 50,000[a] dams with heights greater than 25 ft. or storage volumes in excess of 50 acre-ft. The report also classifies some 20,000 of these as being "so located that failure of the dam could result in loss of human life and appreciable property damage..."

The National Weather Service (NWS) has the responsibility to advise the public of downstream flooding when there is a failure of a dam. Although this type of flood has many similarities to floods produced by precipitation runoff, the dam-break flood has some very important differences which make it difficult to analyze with the common techniques which have worked so well for the precipitation-runoff floods. To aid NWS flash flood hydrologists who are called upon to forecast the

---

[a]Superseded by April 1981 Corps of Engineers National Non-Federal Dam Inventory (66,804) and an additional 3,000 Federal dams.

downstream flooding (flood inundation information and warning times) resulting from dam-failures, a numerical model (DAMBRK) has been recently developed. Herein is presented an outline of the model's theoretical basis, its predictive capabilities, and ways of utilizing the model for forecasting of dam-break floods. The DAMBRK model may also be used for a multitude of purposes by planners, designers, and analysts who are concerned with possible future or historical flood inundation mapping due to dam-break floods and/or reservoir spillway floods, or any specified flood hydrograph.

2. MODEL DEVELOPMENT

The DAMBRK model attempts to represent the current state-of-the-art in understanding of dam failures and the utilization of hydrodynamic theory to predict the dam-break wave formation and downstream progression. The model has wide applicability; it can function with various levels of input data ranging from rough estimates to complete data specification; the required data is readily accessible; and it is economically feasible to use, i.e., it requires a minimal computation effort on large computing facilities.

The model consists of three functional parts, namely: (1) description of the dam failure mode, i.e., the temporal and geometrical description of the breach; (2) computation of the time history (hydrograph) of the outflow through the breach as affected by the breach description, reservoir inflow, reservoir storage characteristics, spillway outflows, and downstream tailwater elevations; and (3) routing of the outflow hydrograph through the downstream valley in order to determine the changes in the hydrograph due to valley storage, frictional resistance, downstream bridges or dams, and to determine the resulting water surface elevations (stages) and flood-wave travel times.

DAMBRK is an expanded version of a practical operational model first presented in 1977 by the author (Fread, 1977). That model was based on previous work by the author on modeling breached dams (Fread and Harbaugh, 1973) and routing of flood waves (Fread, 1974, 1976). There have been a number of other operational dam-break models that have appeared recently in the literature, e.g., Price, et al. (1977), Gundlach and Thomas (1977), Thomas (1977), Keefer and Simons (1977), Chen and Druffel (1977) Balloffet, et al. (1974), Balloffet (1977), Brown and Rogers (1977), Rajar (1978), Brevard and Theurer (1979). DAMBRK differs from each of these models in the treatment of the breach formation, the outflow hydrograph generation, and the downstream flood routing.

2.1 Breach Description

The breach is the opening formed in the dam as it fails. The actual failure mechanics are not well understood for either earthen or concrete dams. In previous attempts to predict downstream flooding due to dam failures, it was usually assumed that the dam failed completely and instantaneously. Investigators of dam-break flood waves such as

Ritter (1892), Schocklitsch (1917), Re (1946), Dressler (1954), Stoker (1957), Su and Barnes (1969), and Sakkas and Strelkoff (1973) assumed the breach encompasses the entire dam and that it occurs instantaneously. Others, such as Schocklitsch (1917) and Army Corps of Engineers (1960), have recognized the need to assume partial rather than complete breaches; however, they assumed the breach occurred instantaneously. The assumptions of instantaneous and complete breaches were used for reasons of convenience when applying certain mathematical techniques for analyzing dam-break flood waves. These assumptions are somewhat appropriate for concrete arch-type dams, but they are not appropriate for earthen dams and concrete gravity-type dams.

Earthen dams which exceedingly outnumber all other types of dams do not tend to completely fail, nor do they fail instantaneously. The fully formed breach in earthen dams tends to have an average width ($\bar{b}$) in the range ($h_d < \bar{b} < 3h_d$) where h_d is the height of the dam. The middle portion of this range for $\bar{b}$ is supported by the summary report of Johnson and Illes (1976). Breach widths for earthen dams are therefore usually much less than the total length of the dam as measured across the valley. Also, the breach requires a finite interval of time for its formation through erosion of the dam materials by the escaping water. Total time of failure may be in the range of a few minutes to a few hours, depending on the height of the dam, the type of materials used in construction, the extent of compaction of the materials, and the extent (magnitude and duration) of the overtopping flow of the escaping water. Piping failures occur when initial breach formation takes place at some point below the top of the dam due to erosion of an internal channel through the dam by escaping water. As the erosion proceeds, a larger and larger opening is formed; this is eventually hastened by caving-in of the top portion of the dam.

Concrete gravity dams also tend to have a partial breach as one or more monolith sections formed during the construction of the dam are forced apart by the escaping water. The time for breach formation is in the range of a few minutes.

Poorly constructed earthen dams and coal-waste slag piles which impound water tend to fail within a few minutes, and have average breach widths in the upper range or even greater than those for the earthen dams mentioned above.

Cristofano (1965) attempted to model the partial, time-dependent breach formation in earthen dams; however, this procedure requires critical assumptions and specification of unknown critical parameter values. Also, Harris and Wagner (1967) used a sediment transport relation to determine the time for breach formation, but this procedure requires specification of breach size and shape in addition to two critical parameters for the sediment transport relation.

For reasons of simplicity, generality, wide applicability, and the uncertainty in the actual failure mechanism, the NWS DAMBRK model allows the forecaster to input the failure time interval (τ) and the terminal size and shape of the breach (Fread and Harbaugh, 1973). The shape (see Fig. 1) is specified by a parameter (z) identifying the side slope of the breach, i.e., 1 vertical: z horizontal slope. The range of z values is: $0 < z < 2$. Rectangular triangular, or trapezoidal shapes may be specified in this way. For example, Z=0 and b>0 produces a trapezoidal shape. The final breach size is controlled by the z parameter and another parameter (b) which is the terminal width of the bottom of the breach. As shown in Fig. 1, the model assumes the breach bottom width starts at a point and enlarges at a linear rate over the failure time interval (τ) until the terminal width is attained and the breach bottom has eroded to the elevation h_{bm} which is usually, but not necessarily, the bottom of the reservoir or outlet channel bottom. If τ is less than 10 minutes, the width of the breach bottom starts at a value of b rather than at a point. This represents more of a collapse failure than an erosion failure.

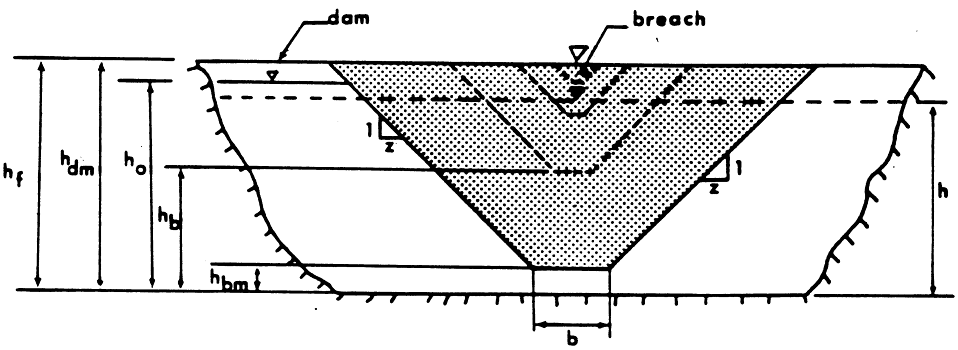

Fig.1- FRONT VIEW OF DAM SHOWING FORMATION OF BREACH

During the simulation of a dam failure, the actual breach formation commences when the reservoir water surface elevation (h) exceeds a specified value, h_f. This feature permits the simulation of an over-topping of a dam in which the breach does not form until a sufficient amount of water is flowing over the crest of the dam. A piping failure may be simulated when h_f is specified less than the height of the dam, h_d.

Selection of breach parameters before a breach forms, or in the absence of observations, introduces a varying degree of uncertainty in the model results; however, errors in the breach description and thence in the resulting time rate of volume outflow are rapidly damped-out as the flood wave advances downstream. For conservative forecasts which err on the side of larger flood waves, values for b and z should produce an average breach width ($\bar{b}$)in the uppermost range for a certain type of dam. Failure time (τ) should be selected in the lower range to produce a maximum outflow. Of course, observational estimates of $\bar{b}$ and τ should be used when available to update forecasts when response time is sufficient as in the case of forecast points several miles downstream of the structure. Flood wave travel rates are often in the range of 2-10 miles per hour. Accordingly, response times for some downstream forecast points may therefore be sufficient for updated forecasts to be issued.

2.2 Reservoir Outflow Hydrograph

The total reservoir outflow consists of broad-crested weir flow through the breach and flow through any spillway outlets, i.e.,

$$Q = Q_b + Q_s \tag{1}$$

The breach outflow (Q_b) is computed as:

$$Q_b = c_1(h-h_b)^{1.5} + c_2)h-h_b)^{2.5} \tag{2}$$

where:

$$c_1 = 3.1\ b_i\ c_v\ k_s \tag{3}$$

$$c_2 = 2.45\ z\ c_v\ k_s \tag{4}$$

$$h_b = h_d - (h_d - h_{bm})\ \frac{t_b}{\tau} \qquad \text{if} \qquad t_b < \tau \tag{5}$$

$$h_b = h_{bm} \qquad \text{if} \qquad t_b > \tau \tag{6}$$

$$b_i = b\ t_b/\tau \qquad \text{if} \qquad t_b < \tau \tag{7}$$

$$c_v = 1.0 + 0.023\ Q^2/[B_d^2\ (h-h_{bm})^2\ (h-h_b)] \tag{8}$$

$$k_s = 1.0 \qquad \text{if} \qquad \frac{h_t - h_b}{h-h_b} < 0.67 \tag{9}$$

otherwise:

$$k_s = 1.0 - 27.8\ \left[\frac{h_t - h_b}{h-h_b} - 0.67\right]^3 \tag{10}$$

in which h_b is the elevation of the breach bottom, h is the reservoir water surface elevation, b_i is the instantaneous breach bottom width, t_b is time interval since breach started forming, c_v is correction for velocity of approach (Brater, 1959), Q is the total outflow from the reservoir, B_d is width of the reservoir at the dam, k_s is the submergence correction for tailwater effects on weir outflow (Benard, 1954), and h_t is the tailwater elevation (water surface elevation immediately downstream of dam).

The tailwater elevation (h_t) is computed from Manning's equation, i.e.,

$$Q = \frac{1.49}{n} S^{1/2} \frac{A^{5/3}}{B^{2/3}} \tag{11}$$

in which n is the Manning roughness coefficient, A is the cross-sectional area of flow, B is the top width of the wetted cross-sectional area, and S is the energy slope. Each term in Eq. (11) applies to a representative channel reach immediately downstream of the dam. The S parameter can be specified by the user; it does not change with time; if it is not specified, the model uses the channel bottom slope of the first third of the downstream valley reach. Since A and B are functions of h_t and Q is the total discharge given by Eq. (1), Eq. (11) provides a sufficiently accurate value for h_t if there are no backwater effects immediately below the dam due to downstream constrictions, dams, bridges, or significant tributary inflows. When these affect the tailwater, Eq. (11) is not used and another procedure, referred to herein as the "simultaneous method," which is described in a following section on multiple dams and bridges is used.

If the breach is formed by piping, Eq. (2)-(9) are replaced by the following orifice flow equation:

$$Q_b = 4.8\ A_p(h-\bar{h})^{1/2} \tag{12}$$

where:

$$A_p = [2b_i+4z(h_f-h_b)]\ (h_f-h_b) \tag{13}$$

$$\bar{h} = h_t \qquad \text{if} \qquad h_t < 2h_f - h_b \tag{14}$$

$$\bar{h} = h_t \qquad \text{if} \qquad h_t > 2h_f - h_b \tag{15}$$

and h_d is replaced by h_f in Eq. (5) to compute h_b.

However, if $\bar{h} - h_f$ and

$$h - h_b < 2.2(h_f-h_b) \tag{16}$$

the flow ceases to be orifice flow and the broad-crested weir flow, Eq. (2), is used.

The spillway outflow (Q_s) is computed as:

$$Q_s = c_s L_s (h-h_s)^{1.5} + c_g A_g (h-h_g)^{0.5} + c_d L_d (h-h_d)^{1.5} + Q_t \qquad (17)$$

in which c_s is the uncontrolled spillway discharge coefficient, h_s is the uncontrolled spillway crest elevation, c_g is the gated spillway discharge coefficient, h_g is the center-line elevation of the gated spillway, c_d is the discharge coefficient for flow over the crest of the dam L_s is the spillway length, A_g is the gate flow area, L_d is the length of the dam crest less L_s, and Q_t is a constant outflow term which is head independent. The uncontrolled spillway flow or the gated spillway flow can also be represented as a table of head-discharge values. The gate flow may also be specified as a function of time.

The total outflow is a function of the water surface elevation (h). Depletion of the reservoir storage volume by the outflow causes a decrease in h which then causes a decrease in Q. However, any inflow to the reservoir tends to increase h and Q. In order to determine the total outflow (Q) as function of time, the simultaneous effects of reservoir storage characteristics and reservoir inflow require the use of a reservoir routing technique. DAMBRK utilizes a hydrologic storage routing technique based on the law of conservation of mass, i.e.,

$$I - Q = dS/dt \qquad (18)$$

in which I is the reservoir inflow, Q is the total reservoir outflow, and dS/dt is the time rate of change of reservoir storage volume. Eq. (18) may be expressed in finite difference form as:

$$(I+I')/2 - (Q+Q')/2 = \Delta S/\Delta t \qquad (19)$$

in which the prime (') superscript denotes values at the time $t-\Delta t$ and the Δ approximates the differential. The term ΔS may be expressed as:

$$\Delta S = (A_s+A_s') (h-h')/2 \qquad (20)$$

in which A_s is the reservoir surface area coincident with the elevation (h).

Combining Eqs. (1), (2), (17), (19) and (20) result in the following expression:

$$(A_s+A_s') (h-h')/\Delta t + c_1(h-h_b)^{1.5} + c_2(h-h_b)^{2.5} + c_s(h-h_b)^{1.5}$$

$$+ c_g(h-h_g)^{0.5} + c_d(h-h_d)^{1.5} + Q_t + Q' - I - I' = 0 \qquad (21)$$

Since A_s is a function of h and all other terms except h are known, Eq. (21) can be solved for the unknown h using Newton-Raphson iteration.

Having obtained h, usually within two or three iterations, Eq. (2) and (17) can be used to obtain the total outflow (Q) at time (t). In this way the outflow hydrograph Q(t) can be developed for each time (t) as t goes from zero to some terminating value (t_e) sufficiently large for the reservoir to be drained. In Eq. (21) the time step (Δt) is chosen sufficiently small to incur minimal numerical integration error. This value is preset in the model to $\tau/50$.

The hydrologic storage routing technique, Eq. (18), implies that the water surface elevation within the reservoir is level. This assumption is quite adequate for gradually occurring breaches with no substantial reservoir inflow hydrographs. However, when 1) the breach is specified to form almost instantaneously so as to produce a negative wage within the reservoir, and/or 2) the reservoir inflow hydrograph is significant enough to produce a positive wave progressing through the reservoir, a routing technique which simulates the negative and/or positive wave(s) occurring within the reservoir could be used for greater accuracy in computing the reservoir outflow through the breach and/or spillways. Such a technique is referred to as dynamic routing. Since this technique is used for routing the dam-break flood wave through the downstream valley, the application of it in lieu of reservoir storage routing will be presented after the downstream routing technique is presented.

2.3 Downstream Routing

After computing the hydrograph of the reservoir outflow, the extent of and time of occurrence of flooding in the downstream valley is determined by routing the outflow hydrograph through the valley. The hydrograph is modified (attenuated, lagged, and distorted) as it is routed through the valley due to the effects of valley storage, frictional resistance to flow, flood wave acceleration components, and downstream obstructions and/or flow control structures. Modifications to the dam-break flood wave are manifested as attenuation of the flood peak elevation, spreading-out or dispersion of the flood wave volume, and changes in the celerity (translation speed) or travel time of the flood wave. If the downstream valley contains significant storage volume such as a wide flood plain, the flood wave can be extensively attenuated and its time of travel greatly increased. Even when the downstream valley approaches that of a uniform rectangular-shaped section, there is appreciable attenuation of the flood peak and reduction in the wave celerity as the wave progresses through the valley.

A distinguishing feature of dam-break waves is the great magnitude of the peak discharge when compared to runoff-generated flood waves having occurred in the past in the same valley. The dam-break flood is usually many times greater than the runoff flood of record. The above-record discharges make it necessary to extrapolate certain coefficients used in various flood routing techniques and make it impossible to fully calibrate the routing technique.

Another distinguishing characteristic of dam-break floods is the very short duration time, and particularly the extremely short time from beginning of rise until the occurrence of the peak. The time to peak is in almost all instances synonymous with the breach formation time (τ) and therefore is in the range of a few minutes to a few hours. This feature, coupled with the great magnitude of the peak discharge, causes the dam-break flood wave to have acceleration components of a far greater significance than those associated with a runoff-generated flood wave.

There are two basic types of flood routing methods, the hydrologic and the hydraulic methods. The hydrologic methods are more of an approximate analysis of the progression of a flood wave through a river reach than are the hydraulic methods. The hydrologic methods are used for reasons of convenience and economy. They are most appropriate as far as accuracy is concerned when the flood wave is not rapidly varying, i.e., the flood wave acceleration effects are negligible compared to the effects of gravity and channel friction. Also, they are best used when the flood waves are very similar in shape and magnitude to previous flood waves for which stage and discharge observations are available for calibrating the hydrologic routing parameters (coefficients).

For routing dam-break flood waves, a particular hydraulic method known as the dynamic wave method is chosen. This choice is based on its ability to provide more accuracy in simulating the dam-break flood wave than that provided by the hydrologic methods, as well as other hydraulic methods such as the kinematic wave and diffusion wave methods. Of the many available hydrologic and hydraulic routing techniques, only the dynamic wave method accounts for the acceleration effects associated with the dam-break waves and the influence of downstream unsteady backwater effects produced by channel constrictions, dams, bridge-road embankments, and tributary inflows. Also, the dynamic wave method can be used economically, i.e., the computational costs can be made insignificant if advantages of certain numerical solution techniques are utilized.

The dynamic wave method based on the complete equations of unsteady flow is used to route the dam-break flood hydrograph through the downstream valley. This method is derived from the original equations developed by Barre De Saint-Venant (1871). The only coefficient that must be extrapolated beyond the range of past experience is the coefficient of flow resistance. It so happens that this is usually not a sensitive parameter in effecting the modifications of the flood wave due to its progression through the downstream valley. The applicability of Saint-Venant equations to simulate abrupt waves such as the dam-break wave has been demonstrated by Terzidis and Strelkoff (1970) and by Martin and Zovne (1971) who used a "through computation" method which ignores the presence of shock waves. DAMBRK uses the "through computation" method as opposed to isolating a single shock wave should it occur, and then applying the shock equations to it and using the Saint-Venant equations for all other portions of the flow.

The Saint-Venant unsteady flow equations consist of a conservation of mass equation, i.e.,

$$\frac{\partial Q}{\partial x} + \frac{\partial(A+A_o)}{\partial t} - q = 0 \tag{22}$$

and a conservation of momentum equation, i.e.,

$$\frac{\partial Q}{\partial x} + \frac{\partial(Q^2/A)}{\partial x} + gA(\frac{\partial h}{\partial x} + S_f + S_e) = 0 \tag{23}$$

where A is the active cross-sectional area of flow, A_o is the inactive (off-channel storage) cross-sectional area, x is the longitudinal distance along the channel (valley), t is the time, q is the lateral inflow or outflow per linear distance along the channel (inflow is positive and outflow is negative in sign), g is the acceleration due to gravity, S_f is the friction slope, and S_e is the expansion-contraction slope. The friction slope is evaluated from Manning's equation for uniform, steady flow, i.e.,

$$S_f = \frac{n^2|Q|Q}{2.21\ A^2\ R^{4/3}} \tag{24}$$

in which n is the Manning coefficient of frictional resistance and R is the hydraulic radius defined as A/B where B is the top width of the active cross-sectional area. The term (S_e) is defined as follows:

$$S_e = \frac{k\ \Delta(Q/A)^2}{2g\ \Delta x} \tag{25}$$

in which k (Morris and Wiggert, 1972) is the expansion-contraction coefficient varying from 0.0 to ±1.0 (+ if contraction, - if expansion), and $\Delta(Q/A)^2$ is the difference in the term $(Q/A)^2$ at two adjacent cross-sections separated by a distance Δx. L is the momentum effect of lateral flow assumed herein to enter or exit perpendicular to the direction of the main flow. This term has the following form: 1) lateral inflow, L = 0; 2) seepage lateral outflow, L = -0.5qQ/A; and 3) bulk lateral outflow, L = -qQ/A.

Eqs. (22)-(23) were modified by the author (Fread, 1975, 1976) and Smith (1978) to better account for the differences in flood wave properties for flow occurring simultaneously in the river channel and the overbank flood plain of the downstream valley. As modified, Eqs. (22)-(23) become:

$$\frac{\partial(K_c Q)}{\partial x_c} + \frac{\partial(K_\ell Q)}{\partial x_\ell} + \frac{\partial(K_r Q)}{\partial x_r} + \frac{\partial A}{\partial t} - q = 0 \tag{26}$$

$$\frac{\partial Q}{\partial t} + \frac{\partial(K_c^2 Q^2/A_c)}{\partial x_c} + \frac{\partial(K_\ell^2 Q^2/A_\ell)}{\partial x_\ell} + \frac{\partial(K_r^2 Q^2/A_r)}{\partial x_r} + gA_c \left[\frac{\partial h}{\partial x_c}\right.$$

$$\left. + S_{fc} + S_e\right] + gA_\ell \left[\frac{\partial h}{\partial x_\ell} + S_{f\ell}\right] + gA_r \left[\frac{\partial h}{\partial x_r} + S_{fr}\right] = 0 \tag{27}$$

in which the subscripts (c), (ℓ), and (r) represent the channel, left flood-plain, and right flood-plain sections, respectively. The parameters (K_c, K_ℓ, K_r) proportion the total flow (Q) into channel flow, left flood-plain flow, and right flood-plain flow, respectively. These are defined as follows:

$$K_c = \frac{1}{1+k_\ell+k_r} \tag{28}$$

$$K_\ell = \frac{k_\ell}{1+k_\ell+k_r} \tag{29}$$

$$K_r = \frac{k_r}{1+k_\ell+k_r} \tag{30}$$

in which

$$k_\ell = \frac{Q_\ell}{Q_c} = \frac{n_c}{n_\ell}\,\frac{A_\ell}{A_c}\,\left[\frac{R_\ell}{R_c}\right]^{2/3}\,\left[\frac{\Delta x_c}{\Delta x_\ell}\right]^{1/2} \tag{31}$$

$$k_r = \frac{Q_r}{Q_c} = \frac{n_c}{n_r}\,\frac{A_r}{A_c}\,\left[\frac{R_r}{R_c}\right]^{1/2}\,\left[\frac{\Delta x_c}{\Delta x_r}\right]^{1/2} \tag{32}$$

Eqs. (31)-(32) represent the ratio of flow in the channel section to flow in the left and right flood-plain (overbank) sections, where the flows are expressed in terms of the Manning equation in which the energy slope is approximated by the water surface slope ($\Delta h/\Delta x$).

The friction slope terms in Eq. (27) are given by the following:

$$S_{fc} = \frac{n_c^2 |K_c Q| K_c Q}{2.21\ A_c^2 R_c^{4/3}} \tag{33}$$

$$S_{f\ell} = \frac{n_\ell^2 |K_\ell Q| K_\ell Q}{2.21\ A_\ell^2 R_\ell^{4/3}} \tag{34}$$

$$S_{fr} = \frac{n_r^2 |K_r Q| K_r Q}{2.21\ A_r^2 R_r^{4/3}} \tag{35}$$

In Eq. (26), the term A is the total cross-sectional area, i.e.,

$$A = A_c + A_\ell + A_r + A_o \tag{36}$$

where A_o is the off-channel storage (inactive) area.

Eqs. (22)-(23) and (26)-(27) constitute a system of partial differential equations of the hyperbolic type. They contain two independent variables, x and t, and two dependent variables, h and Q; the remaining terms are either functions of x, t, h, and/or Q, or they are constants. These equations are not amenable to analytical solutions except in cases where the channel geometry and boundary conditions are uncomplicated and the non-linear properties of the equations are either neglected or made linear. The equations may be solved numerically by performing two basic steps. First, the partial differential equations are represented by a corresponding set of finite difference algebraic equations; and second, the system of algebraic equations is solved in conformance with prescribed initial and boundary conditions.

Eqs. (22)-(23) and (26)-(27) can be solved by either explicit or implicit finite difference techniques (Liggett and Cunge, 1975). Explicit methods, although simpler in application, are restricted by mathematical stability considerations to very small computational time steps (on the order of a few minutes or even seconds). Such small time steps cause the explicit methods to be very inefficient in the use of computer time. Implicit finite difference techniques (Preissmann, 1961; Amein and Fang, 1970; Strelkoff, 1970), however, have no restrictions on the size of the time step due to mathematical stability; however, convergence considerations may require its size to be limited (Fread, 1974a).

Of the various implicit schemes that have been developed, the "weighted four-point" scheme first used by Preissmann(1961), and more recently by Chaudhry and Contractor (1973) and Fread (1974b, 1978) appears most advantageous since it can readily be used with unequal distance steps and its stability-convergence properties can be easily controlled. In the weighted four-point implicit finite difference scheme, the continuous x-t region in which solutions of h and Q are sought, is represented by a rectangular net of discrete points. The net points are determined by the intersection of lines drawn parallel to the x and t axes. Those parallel to the x axis represent time lines; they have a spacing of Δt, which also need not be constant. Each point in the rectangular network can be identified by a subscript (i) which designates the x position and a superscript (j) which designates the time line.

The time derivatives are approximated by a forward difference quotient centered between the i^{th} and i+1 points along the x axis, i.e.,

$$\frac{\partial K}{\partial t} \simeq \frac{K_i^{j+1} + K_{i+1}^{j+1} - K_i^j - K_{i+1}^j}{2\,\Delta t_j} \tag{37}$$

where K represents any variable.

The spatial derivatives are approximated by a forward difference quotient positioned between two adjacent time lines according to weighting factors of Θ and $1-\Theta$, i.e.,

$$\frac{\partial K}{\partial x} \simeq \Theta \left[\frac{K_{i+1}^{j+1} - K_i^{j+1}}{\Delta x_i}\right] + (1-\Theta) \left[\frac{K_{i+1}^j - K_i^j}{\Delta x_i}\right] \tag{38}$$

Variables other than derivatives are approximated at the time level where the spatial derivatives are evaluated by using the same weighting factors, i.e.,

$$K \simeq \Theta \left[\frac{K_i^{j+1} + K_{i+1}^{j+1}}{2}\right] + (1-\Theta) \left[\frac{K_i^j + K_{i+1}^j}{2}\right] \tag{39}$$

A Θ weighting factor of 1.0 yields the fully implicit or backward difference scheme used by Baltzer and Lai (1968). A weighting factor of 0.5 yields the box scheme used by Amein and Fang (1970). The influence of the Θ weighting factor on the accuracy of the computations was examined by Fread (1974a), who concluded that the accuracy decreases as Θ departs from 0.5 and approaches 1.0. This effect becomes more pronounced as the magnitude of the computational time step increases. Usually, a weighting factor of 0.60 is used so as to minimize the loss of accuracy associated with greater values while avoiding the possibility of a weak or pseudo instability noticed by Baltzer and Lai (1968), and Chaudhry and Contractor (1973); however, Θ may be specified other than 0.60 in the data input to the DAMBRK model.

When the finite difference operators defined by Eqs. (37)-(39) are used to replace the derivatives and other variables in Eqs. (22)-(23), the following weighted four-point implicit difference equations are obtained:

$$\Theta \left[\frac{Q_{i+1}^{j+1} - Q_i^{j+1}}{\Delta x_i}\right] - \Theta\, q_i^{j+1} + (1-\Theta) \left[\frac{Q_{i+1}^j - Q_i^j}{\Delta x_i}\right] - (1-\Theta)\, q_i^j$$

$$+ \left[\frac{(A+A_o)_i^{j+1} + (A+A_o)_{i+1}^{j+1} - (A+A_o)_i^j - (A+A_o)_{i+1}^j}{2\Delta t_j}\right] = 0 \tag{40}$$

$$\left(\frac{Q_i^{j+1} + Q_{i+1}^{j+1} - Q_i^j - Q_{i+1}^j}{2\Delta t_j}\right) + \Theta \left[\frac{(Q^2/A)_{i+1}^{j+1} - (Q^2/A)_i^{j+1}}{\Delta x_i} + g\, \bar{A}^{j+1}\right.$$

$$\left.\left(\frac{h_{i+1}^{j+1} - h_i^{j+1}}{\Delta x_i} + \bar{S}_f^{j+1} + S_{ce}^{j+1}\right)\right] + (1-\Theta) \left[\frac{(Q^2/A)_{i+1}^j - (Q^2/A)_i^j}{\Delta x_i}\right.$$

$$\left. + g\, \bar{A}^j \left(\frac{h_{i+1}^j - h_i^j}{\Delta x_i} + \bar{S}_f^j + S_{ce}^j\right)\right] = 0 \tag{41}$$

where:

$$\bar{A} = (A_i + A_{i+1})/2 \tag{42}$$

$$\bar{S}_f = n^2\ \bar{Q}|\bar{Q}|/(2.2\ \bar{A}^2\ \bar{R}^{4/3}) \tag{43}$$

$$\bar{Q} = (Q_i + Q_{i+1})/2 \tag{44}$$

$$\bar{R} = \bar{A}/\bar{B} \tag{45}$$

$$\bar{B} = (B_i + B_{i+1})/2 \tag{46}$$

The terms associated with the j^{th} time line are known from either the initial conditions or previous computations. The initial conditions refer to values of h and Q at each node along the x axis for the first time line (j=1).

Eqs. (40)-(41) cannot be solved in an explicit or direct manner for the unknowns since there are four unknowns and only two equations. However, if Eqs. (40)-(41) are applied to each of the (N-1) rectangular grids between the upstream and downstream boundaries, a total of (2N-2) equations with 2N unknowns can be formulated. (N denotes the total number of nodes). Then, prescribed boundary conditions, one at the upstream boundary and one at the downstream boundary, provide the necessary two additional equations required for the system to be determinate. The resulting system of 2N non-linear equations with 2N unknowns is solved by a functional iterative procedure, the Newton-Raphson method (Amein and Fang, 1970).

Computations for the iterative solution of the non-linear system are begun by assigning trial values to the 2N unknowns. Substitution of the trial values into the system of non-linear equations yields a set of 2N residuals. The Newton-Raphson method provides a means for correcting the trial values until the residuals are reduced to a suitable tolerance level. This is usually accomplished in one or two iterations through use of linear extrapolation for the first trial values. If the Newton-Raphson corrections are applied only once, i.e., there is no iteration, the non-linear system of difference equations degenerates to the equivalent of a quasi-linear formulation which may require smaller time steps than the non-linear formulation for the same degree of numerical accuracy.

A system of 2N x 2N linear equations relates the corrections to the residuals and to a Jacobian coefficient matrix composed of partial derivatives of each equation with respect to each unknown variable in that equation. The coefficient matrix of the linear system has a banded structure which allows the system to be solved by a compact quad-diagonal Gaussian elimination algorithm (Fread, 1971), which is very efficient with respect to computing time and storage. The required storage is 2N x 4 and the required number of computational steps is approximately 38N.

The DAMBRK model has the option to use either Eqs. (22)-(23) or Eqs. (26)-(27). The former is a somewhat simpler treatment in which a total or composite cross-section is used, whereas the latter set utilizes a more detailed representation of the flow cross-section. Eqs. (26)-(27) are recommended when the channel is sufficiently large to carry a significant portion of the total flow and the channel has a rather meandrous path through the downstream valley.

2.4 Initial and Boundary Conditions

In order to solve the unsteady flow equations the state of the flow (h and Q) must be known at all cross-sections at the beginning (t=0) of the simulation. This is known as the initial condition of the flow. The DAMBRK model assumes the flow to be steady, non-uniform flow where the flow at each cross-section is initially computed to be:

$$Q_i = Q_{i-1} + q_{i-1}\,\Delta x_{i-1} \qquad i=2,3,\ldots N \tag{47}$$

where Q_1 is the known steady discharge at the dam, i.e., the upstream boundary of the downstream valley, and q_i is any lateral inflow from tributaries existing between the cross-sections spaced at intervals of Δx along the valley. The steady discharge from the dam at t=0 must be non-zero, i.e., a dry downstream channel is not amenable to simulation by DAMBRK. This is not an important restriction, especially when maximum flows and peak stages are of paramount interest in the dam-break flood. The tributary lateral inflow must be specified by the forecaster throughout the simulation period. If these flows are relatively small, they may be safely ignored.

The water surface elevations associated with the steady flow must also be computed at t=0. This is accomplished by solving the following equation:

$$\frac{(Q^2/A)_{i+1} - (Q^2/A)_i}{\Delta x_i} + g\left[\frac{A_i+A_{i+1}}{2}\right]\left[\frac{h_{i+1}-h_i}{\Delta x_i}\right.$$

$$\left. + \frac{n^2(Q_i+Q_{i+1})^2\ (B_i+B_{i+1})^{4/3}}{2.2\ (A_i+A_{i+1})^{10/3}}\right] = 0 \tag{48}$$

This equation may be easily solved using the Newton-Raphson method by starting at a specified elevation at the downstream extremity of the valley and solving for the adjacent upstream elevation step by step until the upstream boundary is reached. The downstream specified elevation may be obtained from a solution of the Manning equation if the flow is governed only by the channel conditions; however, if a flow control structure produces a back-up of the flow at this location, the forecaster must directly specify the water surface elevation existing at the downstream boundary at t=0.

In addition to initial conditions, boundary conditions at the upstream and downstream sections of the valley must be specified for all times ($t=0$ to $t=t_e$ where t_e is the future time at which the simulation ceases).

At the upstream boundary the reservoir outflow hydrograph Q(t) provides the necessary boundary condition.

At the downstream boundary an appropriate stage-discharge relation is used. If the flow at the downstream extremity is channel-controlled, the following relation is used:

$$Q_N = \frac{1.49}{n} A_N^{5/3}/B_N^{2/3} \left[\frac{h_{N-1}-h_N}{\Delta x_{N-1}}\right]^{1/2} \tag{49}$$

Eq. (49) reproduces the hysteresis effect in stage-discharge relations often observed as a loop-rating curve. The loop (hysteresis) is produced by the temporal variations in the water surface slope. If the flow at the downstream boundary is controlled by a flow control structure such as a dam, the following relation is used:

$$Q_N = Q_b + Q_s \tag{50}$$

where the breach flow (Q_b) is defined by Eq. (2) and the spillway flow (Q_s) is defined by Eq. (17) in which the various terms apply to the dam at the downstream boundary. Since the resulting expressions for Q_b and Q_s are in terms of the water surface elevation, h_N, Eq. (50) is a stage-discharge relation.

The downstream boundary condition may also be specified as a single-value rating curve in which the stage-discharge values are input as tabular values. Linear interpolation is used for determining intermediate values. The downstream boundary may also be a known water surface elevation as a function of time, e.g., a tidal condition.

2.5 Multiple Dams and Bridges

The DAMBRK model can simulate the progression of a dam-break wave through a downstream valley containing a reservoir created by another downstream dam, which itself may fail due to being sufficiently overtopped by the wave produced by the failure of the upstream dam. In fact, an unlimited number of reservoirs located sequentially along the valley can be simulated. In DAMBRK there is a choice of two methods for simulating dam-break flows in a valley having multiple dams.

In the first method, which is known as the "sequential method," the downstream boundary condition for the dynamic routing component is given by Eq. (50) rather than Eq. (49). The properties of the downstream dam, spillways, breach description, and elevation of flow which precipitates the failure of the dam, are used in Eq. (50). In this way, backwater effects of the downstream dam are included in the routing of the outflow hydrograph from the upstream dam. The most upstream reservoir may be simulated using either storage or dynamic routing.

When the tailwater below a dam is affected by flow conditions downstream of the tailwater section (e.g., backwater produced by a downstream dam, flow constriction, bridge, and/or tributary inflow), the flow occurring at the dam is computed by the second method known as the "simultaneous method" which uses an internal boundary condition at the dam. In this method the dam is treated as a short Δx reach in which the flow through the reach is governed by the following two equations rather than either Eqs. (22)-(23) or Eqs. (26)-(27):

$$Q_i = Q_{i+1} \tag{51}$$

$$Q_i = Q_b + Q_s \tag{52}$$

in which Q_b and Q_s are breach flow and spillway flow as described in Eqs. (2) and (17). In this way the flows, Q_i and Q_{i+1}, and the elevations, h_i and h_{i+1}, are in balance with the other flows and elevations occurring simultaneously throughout the entire flow system; the system may consist of additional dams which are treated as additional internal boundary conditions via Eqs. (51)-(52). Either storage or dynamic routing may be used in the most upstream reservoir. This method can also be used for a flow system having a single dam, only.

Highway/railway bridges and their associated earthen embankments which are located at points downstream of a dam may also be treated as internal boundary conditions. Eqs. (51)-(52) are used at each bridge; the term Q_s in Eq. (52) is computed by the following expression:

$$Q_s = 8.02\ C\ A_{i+1}(h_i-h_{i+1})^{1/2} + cc_u\ L_u\ k_u(h_i-h_{cu})^{3/2}$$

$$+\ cc_\ell\ L_\ell\ k_\ell(h_i-h_{c\ell})^{3/2} \tag{53}$$

in which

$$k_u = 1.0 \qquad \text{if} \qquad h_{ru} < 0.76 \tag{54}$$

valley can be simulated. In DAMBRK there is a choice of two methods for simulating dam-break flows in a valley having multiple dams.

In the first method, which is known as the "sequential method," the downstream boundary condition for the dynamic routing component is given by Eq. (50) rather than Eq. (49). The properties of the downstream dam, spillways, breach description, and elevation of flow which precipitates the failure of the dam, are used in Eq. (50). In this way, backwater effects of the downstream dam are included in the routing of the outflow hydrograph from the upstream dam. The most upstream reservoir may be simulated using either storage or dynamic routing.

When the tailwater below a dam is affected by flow conditions downstream of the tailwater section (e.g., backwater produced by a downstream dam, flow constriction, bridge, and/or tributary inflow), the flow occurring at the dam is computed by the second method known as the "simultaneous method" which uses an internal boundary condition at the dam. In this method the dam is treated as a short Δx reach in which the flow through the reach is governed by the following two equations rather than either Eqs. (22)-(23) or Eqs. (26)-(27):

$$Q_i = Q_{i+1} \tag{51}$$

$$Q_i = Q_b + Q_s \tag{52}$$

in which Q_b and Q_s are breach flow and spillway flow as described in Eqs. (2) and (17). In this way the flows, Q_i and Q_{i+1}, and the elevations, h_i and h_{i+1}, are in balance with the other flows and elevations occurring simultaneously throughout the entire flow system; the system may consist of additional dams which are treated as additional internal boundary conditions via Eqs. (51)-(52). Either storage or dynamic routing may be used in the most upstream reservoir. This method can also be used for a flow system having a single dam, only.

Highway/railway bridges and their associated earthen embankments which are located at points downstream of a dam may also be treated as internal boundary conditions. Eqs. (51)-(52) are used at each bridge; the term Q_s in Eq. (52) is computed by the following expression:

$$Q_s = 8.02\ C\ A_{i+1}(h_i-h_{i+1})^{1/2} + cc_u\ L_u\ k_u(h_i-h_{cu})^{3/2}$$

$$+\ cc_\ell\ L_\ell\ k_\ell(h_i-h_{c\ell})^{3/2} \tag{53}$$

in which

$$k_u = 1.0 \qquad \text{if} \qquad h_{ru} < 0.76 \tag{54}$$

A modified compact quad-diagonal Gaussian elimination algorithm similar to the one previously described is required for solving the unsteady flow equations when supercritical flow exists. The modification results when the form of the Jacobian coefficient matrix is slightly changed due to the need for two upstream boundary conditions and none at the downstream boundary.

The DAMBRK model is constructed to accommodate supercritical flow for either the entire channel reach or for only an upstream portion of the entire reach. The supercritical flow regime is assumed to be applicable throughout the duration of the flow. Multiple reservoirs on supercritical valley slopes must be treated using a storage routing technique such as Eq. (18) rather than the dynamic routing technique.

2.7 Routing Losses

Often in the case of dam-break floods, where the extremely high flows inundate considerable portions of channel overbank or valley flood plain, a measurable loss of flow volume occurs. This is due to infiltration into the relatively dry overbank material, detention storage losses, and sometimes short-circuiting of flows from the main valley into other drainage basins via canals or overtopping natural ridges separating the drainage basins. Such losses of flow may be taken into account via the term q in Eq. (22) or Eq. (26). An expression describing the loss is given by the following:

$$q_m = -0.00458\ V_L\ P/(L\ \bar{T}) \tag{63}$$

in which V_L is the outflow volume (acre-ft) from the reservoir; P is the volume loss ratio; L is the length (mi) of downstream channel through which the loss occurs; and T is the average duration (hr) of the flood wave throughout the reach length L; and q_m is the maximum lateral outflow (cfs/ft) occurring along the reach L throughout the duration of flow. The mean lateral outflow is proportioned in time and distance along the reach L such that $q_i^j=0$ when $Q_i^j=Q_i^1$ and $q_i^j=q_m$ when $Q_i^j=Q_{max_i}$. Thus:

$$q_i^j = \frac{(Q_i^j-Q_i^1)}{(Q_{max_i}-Q_i^1)}\ q_m \tag{64}$$

$$Q_{max_i} = Q_{max_N} + (Q_{max}-Q_{max_N})\ \left(\frac{X_N - X_i}{L}\right)^m \tag{65}$$

where Q_i^1 is the initial flow, Q_{max_i} is the estimated maximum flow at each flood node, Q_{max_N} is the maximum routed discharge at the downstream section (X_n), Q_{max} is the maximum discharge at the dam and m is a fitted exponent. The parameter P may vary from only a few percent to more than 30, depending on the conditions of the downstream valley.

2.8 Tributary Inflows/Outflows

Unsteady flows associated with tributaries downstream of the dam can be added to the unsteady flow resulting from the dam failure. This is accomplished via the term q in Eq. (22) or Eq. (26). The tributary flow is distributed along a single Δx reach. Backwater effects of the dam-break flow on the tributary flow are ignored, and the tributary flow is assumed to enter perpendicular to the dam-break flow. Outflows are assigned negative values. Outflows which occur as broad-crested weir flow over a levee or natural crest may be simulated. The crest elevation, discharge coefficient, and location along the river-valley must be specified. The head is computed as the average water surface elevation, along the length of the crest, less the crest elevation.

2.9 Floodplain Compartments

The DAMBRK model can simulate the exchange of flow between the river and floodplain compartments. The floodplain compartments are formed by a levee which runs parallel to the river on either or both sides of the river, and other levees or road embankments which run perpendicular to the river. Flow transfer between a floodplain compartment and the river is assumed to occur along one Δx reach and is controlled by broad-crested weir flow with submergence correction. Flow can be either away from the river or into the river, depending on the relative water surface elevations of the river and the floodplain compartment. The river elevations are computed via Eqs. (40-41), and the floodplain water surface elevations are computed by a simple storage routing relation, i.e.,

$$V_\ell^{t} = V_\ell^{t-\Delta t} + \left(I^t - O^t\right) \Delta t/43560 \tag{66}$$

in which V_ℓ is the volume (acre-ft) in the floodplain compartment at time t or $t-\Delta t$ referenced to the water elevation, I is the inflow from the river or adjacent floodplain compartments, and O is the outflow from the floodplain compartment to the river and/or to adjacent floodplain compartments. Flow transfer between adjacent floodplain compartments is also controlled by broad-crested weir flow with submergence correction. The broad-crested weir flow is according to the following:

$$I = c\ s_b\ \left(h_r - h_{fp}\right)^{3/2} \tag{67}$$

$$O = c\ s_b\ \left(h_{fp} - h_r\right)^{3/2} \tag{68}$$

in which c is a specified discharge coefficient, h_r is the river elevation, h_{fp} is the water surface elevation of the floodplain, and s_b is the submergence correction factor, i.e.

$$s_b = 1.0 \qquad h_r < 0.67 \qquad (69)$$

$$s_b = 1.0 - 27.8 \left(H_r - 0.67\right)^3 \qquad h_r > 0.67 \qquad (70)$$

$$H_r = \left(h_r - h_w\right)/\left(h_{fp} - h_w\right) \qquad (71)$$

and h_w is the specified elevation of the crest of the levee. The floodplain elevation $\left(h_{fp}\right)$ is obtained iteratively via a table look-up algorithm from the specified table of volume-elevation values. The outflow from a floodplain compartment may also include that from one or more pumps associated with each floodplain compartment. Each pump has a specified discharge-head relation given in tabular form along with start-up and shut-off operation instructions depending on specified water surface elevations. The pumps discharge to the river.

2.10 Reservoir Dynamic Routing

As mentioned earlier, an option is provided in the DAMBRK model to use dynamic routing rather than storage routing to compute the reservoir outflow hydrograph. The dynamic routing is identical to the above description with the exception of boundary conditions. The upstream boundary condition is a discharge hydrograph given by the following:

$$Q_1^{j+1} - I(t) = 0 \qquad (72)$$

where I(t) is the known reservoir inflow hydrograph. The downstream boundary condition is a stage-discharge relation given by Eq. (50). The initial water surface elevations are computed by solving Eq. (48), the steady gradually varied backwater equation, using h_o which is the elevation of the water surface at the dam site when the computation commences. The reservoir dynamic routing procedure must contend with the lowering of the water surface elevation at the upstream boundary as the reservoir volume is depleted by the outflow through the breach. If this depth becomes small and approaches a value less than the normal depth, the computations become unstable. To avoid this computational problem, the upstream depth is constantly monitored; if it becomes less than the initial normal depth (d_n), the location of the upstream boundary condition is shifted downstream one node at a time until the depth at the node is greater than d_n.

2.11 Landslide-Generated Waves

Reservoirs are sometimes subject to landslides which rush into the reservoir, displacing a portion of the reservoir contents and, thereby, creating a very steep water wave which travels up and down the length of the reservoir (Davidson and McCartney, 1975). This wave may have sufficient amplitude to overtop the dam and precipitate a failure of the dam, or the wave by itself may be large enough to cause catastrophic flooding downstream of the dam without resulting in the failure of the dam as perhaps in the case of a concrete dam such as the Viaont Dam flood of 1963.

The capability to generate waves produced by landslides is provided within DAMBRK. The volume of the landslide mass, its porosity, and time interval over which the landslide occurs, are input to the model. In the model, the landslide mass is deposited within the reservoir in layers during small computational time steps, and simultaneously the original dimensions of the reservoir are reduced accordingly. The time rate of reduction in the reservoir cross-sectional area (Koutitas, 1977) creates the wave during the solution of the unsteady flow, Eqs. (22)-(23), which are applied to the cross-sections describing the reservoir characteristics. The upstream boundary condition is given by Eq. (72), and the downstream boundary condition is given by Eq. (50). The initial conditions are obtained as described by Eqs. (47)-(48) for steady non-uniform flow.

Wave runup is not considered in the model. For near vertical faces of concrete dams the runup may be neglected; however, for earthen dams the angle of the earth fill on the reservoir side will result in a surge which will advance up the face of the dam to a height approximately equal to 2.5 times the height of the landslide-generated wave (Morris and Wiggert, 1972).

2.12 Selection of Δt and Δx

Rapidly rising hydrographs, such as the dam-break outflow hydrograph, can cause computational problems (instability and non-convergence) when applied to numerical approximations of the unsteady flow equations. This is the case even when an implicit, non-linear finite difference solution technique is used. However, many computational problems can be overcome by proper selection of time step (Δt) size. During the limited testing of the model presented herein, two types of computational problems arose. First, if the time step were too large relative to the rate of increase of discharge during that time step, errors occurred in the computed water surface elevation in the vicinity of the wave front. These water surface elevations would tend to dip toward the channel bottom and quickly cause negative areas to be computed which would then cause the computations to "blow up." Second, too large a time step would also cause the Newton-Raphson iteration to not converge. The first computational problem is similar to that experienced by Cunge (1975). Both of the computational problems were successfully treated by reducing the time step size by a factor of 0.5 whenever negative areas were computed, or when a reasonable number of iterations were exceeded. With the reduced time step, the computations were repeated. If the same problems persisted, the time step was again halved and the computations repeated. Usually, one or two reductions would be sufficient. The computational process was then advanced to the next time level by the original unreduced time step. Computations were initially begun with Δt time steps (hr) computed via the following relation:

$$\Delta t = \tau/M \tag{73}$$

in which τ is the time (hr) from the beginning of rise to the peak of the outflow hydrograph and M is the divisor for determining the time step. A reasonable value for M is 20 for subcritical flow and 40 for supercritical flow.

Distance steps (Δx) are selected in the following range:

$$\Delta x \leq c \ \Delta t \tag{74}$$

where c is the wave speed in mi/hr and Δx is in miles. The dam-break hydrograph tends to be a very peaked-type of hydrograph and, as such, tends to dampen and flatten out as it advances downstream. Accordingly, the time step may be increased as the wave progresses downstream; therefore, smaller values of Δx are selected immediately downstream of the dam, with a gradual increase in size at greater distances downstream of the dam. Also, the smaller values of Δx are associated with the smaller values of τ. This methodology of selecting Δx and Δt values follows the guidelines set forth in an analysis made by Fread (1974a) of the numerical properties of the four-point implicit solution of the unsteady flow equations.

Distance steps may need to be reduced in size where severe expansions or contractions in the cross sections occur.

Since the flood wave dampens out as it moves downstream, the Δt time step may be increased as the computations advance in time. The following scheme is used:

$$\Delta t = T_p/M \qquad\qquad t \leq t_b + 2\tau \tag{75}$$

where T_p is the time between the start of rise of the hydrograph and the peak of the hydrograph at selected locations along the downstream valley. Six evenly spaced locations along the downstream valley commencing at the dam site are monitored to determine T_p. The peak must have occurred at one of the locations before T_p can be evaluated. Since T_p increases at locations farther and farther downstream of the dam, the T_p which exists for the most downstream location is used in Eq. (75). An option exists to maintain throughout the computations and time step size specified in the data input. The units of Δt, t_b, and T_p are hours.

3. DATA REQUIREMENTS

The DAMBRK model was developed so as to require data that was accessible to the forecaster. The input data requirements are flexible insofar as much of the data may be ignored (left blank on the input data cards or omitted altogether) when a detailed analysis of a dam-break flood inundation event is not feasible due to lack of data or insufficient data preparation time. Nonetheless, the resulting approximate analysis is more accurate and convenient to obtain than that which could be computed by other techniques. The input data can be categorized into two groups.

The first data group pertains to the dam (the breach, spillways, and reservoir storage volume). The breach data consists of the following parameters: τ (failure time of breach, in hours); b (final bottom width of breach); z (side slope of breach); h_{bm} (final elevation of breach bottom); h_o (initial elevation of water in reservoir); h_f (elevation of water when breach begins to form); and h_d (elevation of top of dam). The spillway data consists of the following: h_s (elevation of uncontrolled spillway crest); c_s (coefficient of discharge of uncontrolled spillway); h_g (elevation of center of submerged gated spillway); c_g (coefficient of discharge of gated spillway); c_d (coefficient of discharge of crest of dam); and Q_t (constant, head independent discharge from dam). The storage parameters consist of the following: a table of surface area (A_s) in acres or volume in acre-ft. and the corresponding elevations within the reservoir. The forecaster must estimate the values of τ b, z, h_{bm}, and h_f. The remaining values are obtained from the physical description of the dam, spillways, and reservoir. In some cases h_s, c_s, h_g, c_g, and c_d may be ignored and Q_t used in their place.

The second group pertains to the routing of the outflow hydrograph through the downstream valley. This consists of a description of the cross-sections, hydraulic resistance coefficients, and expansion coefficients. The cross-sections are specified by location mileage, and tables of top width (active and inactive) and corresponding elevations. The active top widths may be total widths as for a composite section, or they may be left flood-plain, right flood-plain, and channel widths. The top widths can be obtained from USGS topography maps, 7 1/2' series, scale 1:24000. The channel widths are usually not as significant for an accurate analysis as the overbank widths (the latter are available from the topo maps). The number of cross-sections used to describe the downstream valley depends on the variability of the valley widths. A minimum of two must be used. Additional cross-sections are created by the model via linear interpolation between adjacent cross-sections specified by the forecaster. This feature enables only a minimum of cross-sectional data to be input by the forecaster according to such criteria as data availability, variation, preparation time, etc. The number of interpolated cross-sections created by the model is controlled by the parameter DXM which is input for each reach between specified cross-sections. The hydraulic resistance coefficients consist of a table of Manning's n vs. elevation for each reach between specified cross-sections. The expansion-contraction coefficients (k) are specified as non-zero values at sections where significant expansion or contractions occur. The k parameters may be left blank in most analyses.

4. MODEL TESTING

The DAMBRK model has been tested on five historical dam-break floods to determine its ability to reconstitute observed downstream peak stages, discharges, and travel times. Those floods that have been used in the testing are: 1976 Teton Dam, 1972 Buffalo Creek Coal-WAste Dam, 1889 Johnstown Dam, 1977 Toccoa (Kelly Barnes) Dam, and the 1977 Laurel Run Dam floods. However, only the Teton and Buffalo Creek floods will be presented herein.

4.1 Teton Dam Flood

The Teton Dam, a 300 ft. high earthen dam with a 3,000 ft. long crest and 250,000 acre-ft of stored water, failed on June 5, 1976, killing 11 people, making 25,000 homeless, and inflicting about \$400 million in damages to the downstream Teton-Snake River Valley. Data from a Geological Survey Report by Ray, et al. (1977) provided observations on the approximate development of the breach, description of the reservoir storage, downstream cross-sections and estimates of Manning's n approximately every 5 miles, indirect peak discharge measurements at 3 sites, flood-peak travel times, and flood-peak elevations. The inundated area is shown in Fig. 2.

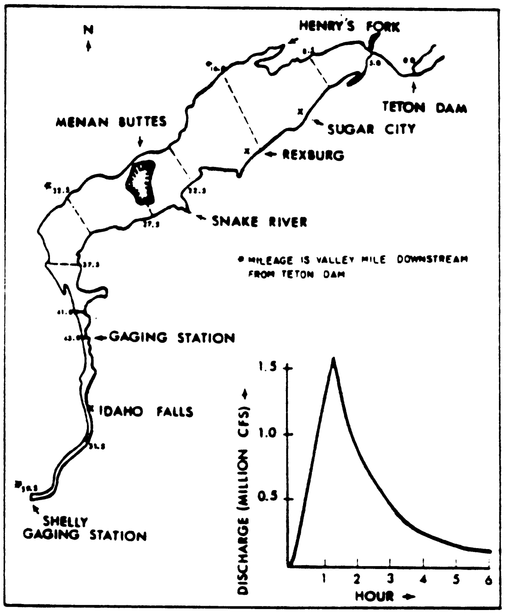

Fig. 2 – OUTFLOW HYDROGRAPH AND FLOODED AREA DOWNSTREAM OF TETON DAM

The following breach parameters were used in DAMBRK to reconstitute the downstream flooding due to the failure of Teton Dam: τ = 1.25 hrs., b = 150 ft., z = 0, h_{bm} = 0.0, $h_f = h_d = h_o$ = 261.5 ft. Cross-sectional properties at 12 locations shown in Fig. 2 along the 60-mile reach of the Teton-Snake River Valley below the dam were used. Five top widths were used to describe each cross-section. The downstream valley consisted of a narrow canyon (approx. 1,000 ft. wide) for the first 5 miles and thereafter a wide valley which was inundated to a width of about 9 miles. Manning's n values ranging from 0.028 to 0.047 were provided from field estimates by the Geological Survey. DXM values between cross-sections were assigned values that gradually increased from 0.5 miles near the dam, to a value of 1.5 miles near the downstream boundary at the Shelly gaging station (valley mile 59.5 downstream from the dam). The reservoir surface area-elevation values were obtained from Geological Survey topo maps. The downstream boundary was assumed to be channel flow control as represented by a loop rating curve given by Eq. (49).

The computed outflow hydrograph is shown in Fig. 2. It has a peak value of 1,652,300 cfs (cubic feet per second), a time to peak of 1.25 hrs., and a total duration of about 6 hours. This peak discharge is about 20 times greater than the flood of record at Idaho Falls. The temporal variation of the computed outflow volume compared within 5 percent of observed values as shown in Fig. 3. In Fig. 4 a comparison

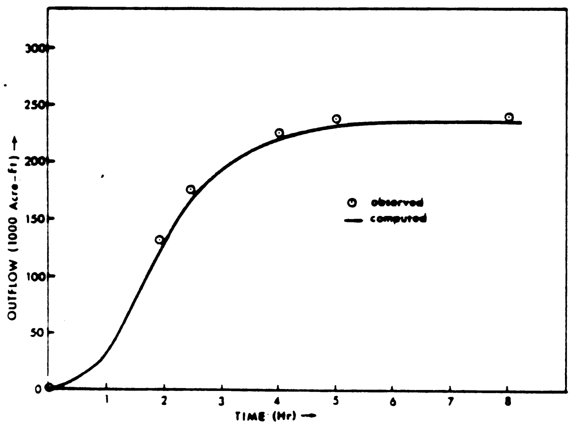

Fig. 3 - OUTFLOW VOLUME FROM TETON DAM

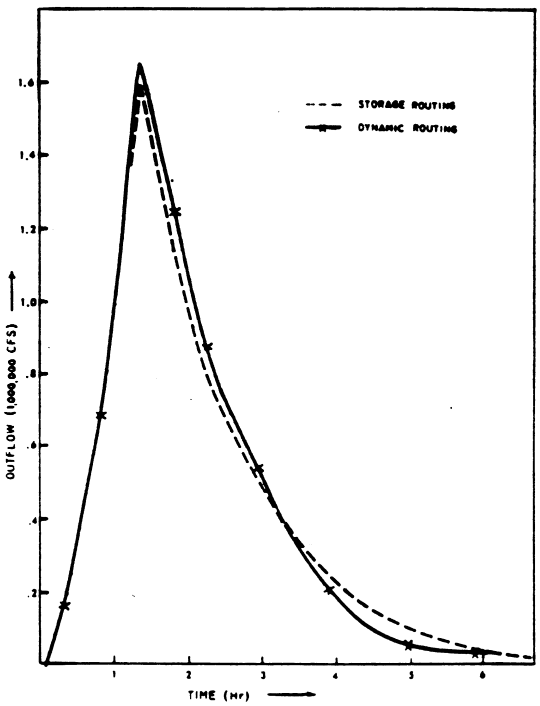

Fig. 4 - OUTFLOW HYDROGRAPH FROM TETON DAM FAILURE

is presented of Teton reservoir outflow hydrographs computed via reservoir storage routing and reservoir dynamic routing. Since the breach of the Teton Dam formed gradually over approximately a one-hour interval, a steep negative wave did not develop. Also, the inflow to the reservoir was not very significant. For these two reasons, the reservoir surface remained essentially level during the reservoir drawdown and the dynamic routing yielded almost the same outflow hydrograph as the level pool, storage routing technique.

The computed peak discharge values along the 60-mile downstream valley are shown in Fig. 5 along with three observed (indirect measurement) values at miles 8.5, 43.0, and 59.5. The average difference between the computed and observed values is 4.8 percent. Most apparent is the extreme attenuation of the peak discharge as the flood wave progresses through the valley. Two computed curves are shown in Fig. 5; one in which no losses were assumed, i.e., $q_m = 0$; and a second in which the losses were assumed to vary from zero to a maximum of $q_m = -0.30$ cfs/ft and were accounted for the model through the q term in Eq. (22). Losses were due to infiltration and detention storage behind irrigation levees amounting to about 25 percent of the reservoir outflow volume. Eq. (63) was used to compute q_m.

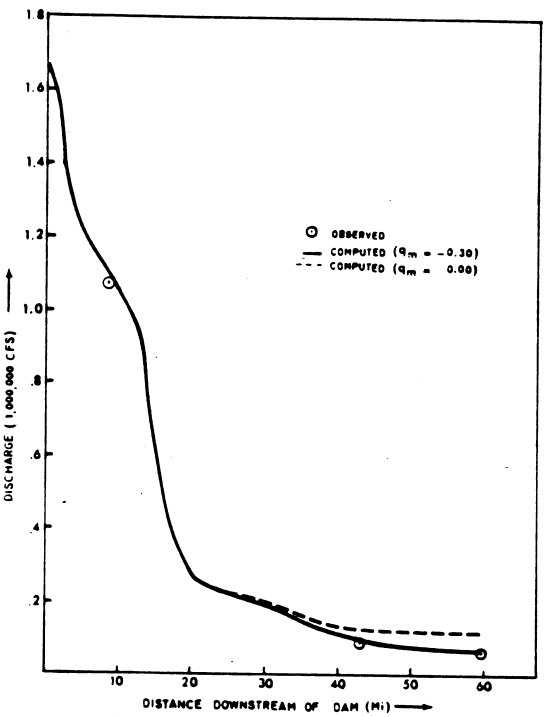

Fig. 5 - PROFILE OF PEAK DISCHARGE FROM TETON DAM FAILURE

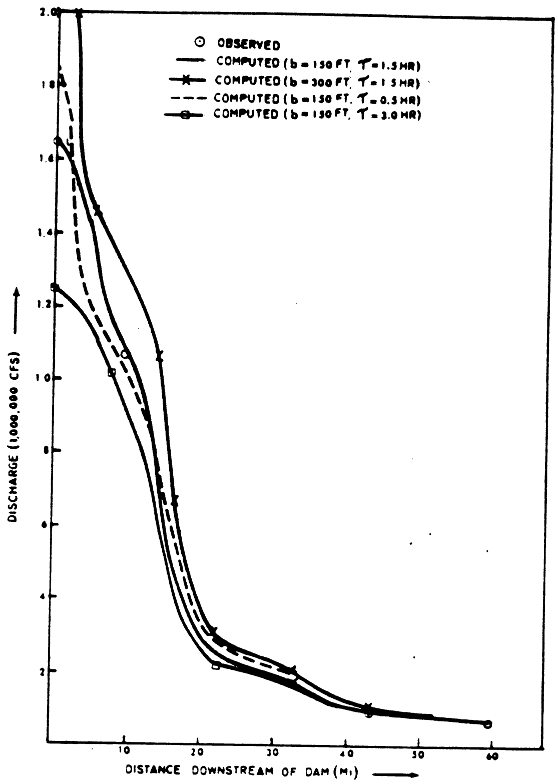

Fig. 6 - PROFILE OF PEAK DISCHARGE FROM TETON DAM FAILURE SHOWING SENSITIVITY OF VARIOUS INPUT PARAMETERS

The a priori selection of the breach parameters (τ and b) causes the greatest uncertainty in forecasting dam-break flood waves. The sensitivity of downstream peak discharges to reasonable variations in τ and b are shown in Fig. 6. Although there are large differences in the discharges (+45 to -25 percent) near the dam, these rapidly diminish in the downstream direction. After 10 miles the variation is +20 to -14 percent, and after 15 miles the variation has further diminished (+15 to -8 percent). The tendency for extreme peak attenuation and rapid damping of differences in the peak discharge is accentuated in the case of Teton Dam due to the presence of the very wide valley. Had the narrow canyon extended all along the 60-mile reach to Shelly, the peak discharge would not have attenuated as much and the differences in peak discharges due to variations in τ and $\bar{b}$ would be more persistent. In this instance, the peak discharge would have attenuated to about 350,000 rather than 67,000 as shown in Fig. 6, and the differences in peak discharges at mile 59.5 would have been about 27 percent as opposed to less than 5 percent as shown in Fig. 6.

Computed peak elevations compared favorably with observed values, as shown in Fig. 7. The average absolute error was 1.5 ft., while the average arithmetic error was only -0.2 ft.

The computed flood-peak travel times and three observed values are shown in Fig. 8. The differences between the computed and observed are about 10 percent for the case of using the estimated Manning's n values and about 1 percent if the n values are slightly increased by 7 percent.

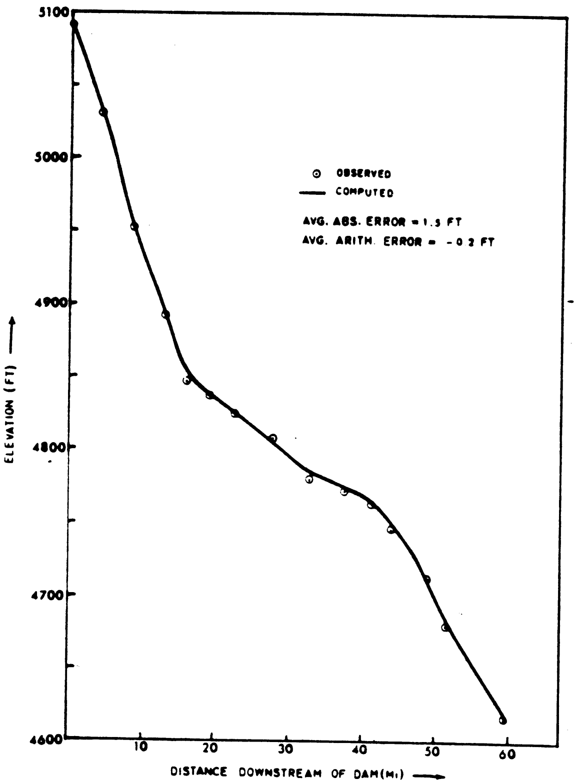

Fig. 7 — PROFILE OF PEAK FLOOD ELEVATION FROM TETON DAM FAILURE

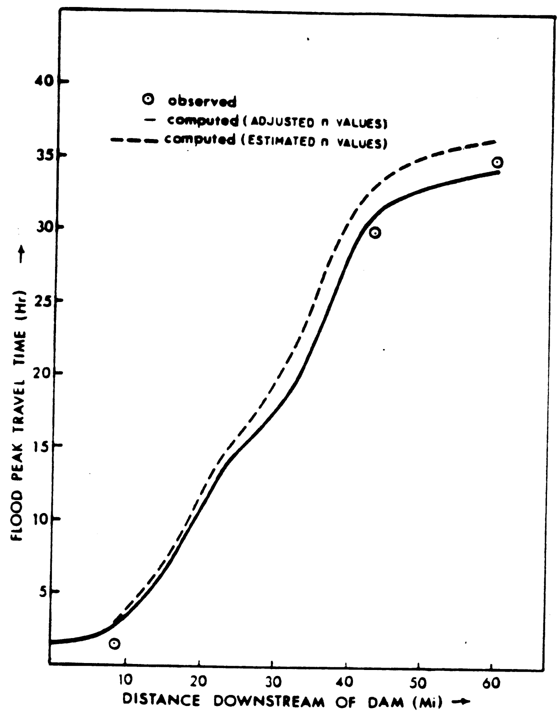

Fig. 8 — TRAVEL TIME OF FLOOD PEAK FROM TETON DAM FAILURE

As mentioned previously, the Manning's n must be estimated, especially for the flows above the flood of record. The sensitivity of the computed states and discharges of the Teton flood due to a substantial change (20 percent) in the Manning's n was found to be as follows: 1) 0.5 ft in computed peak water surface elevations or about 2 percent of the maximum flow depths, 2) 16 percent deviation in the computed peak discharges, 3) 0.8 percent change in the total attenuation of peak discharge incurred in the reach from Teton Dam to Shelly, and 4) 15 percent change in the flood-peak travel time at Shelly. These results indicate that Manning's n has little effect on peak elevations or depths; however, the travel time is affected by nearly the same percent that the n values are changed.

A typical simulation of the Teton flood as described above involved 78 Δx reaches, 55 hrs. of prototype time, and an initial time step (Δt) of 0.06 hrs. Such a simulation run required only 19 seconds of CPU time on an IBM 360/195 computer system; the associated cost was less than $5 per run.

4.2 Buffalo Creek Flood

The DAMBRK model was also applied to the failure of the Buffalo Creek coal-waste dam which collapsed on the Middle Fork, a tributary of Buffalo Creek (See Fig. 9) in southwestern West Virginia near Saunders. The dam failed very rapidly on February 26, 1972, and released about

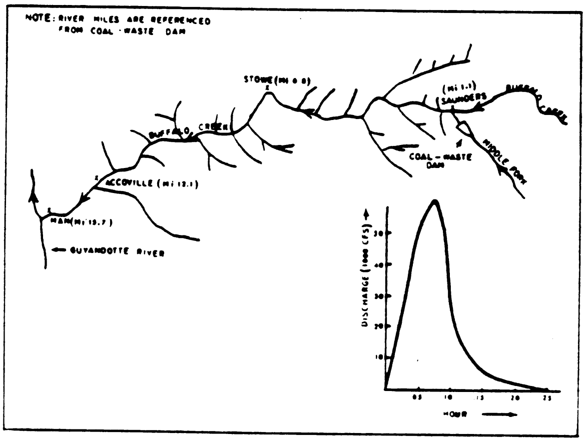

Fig. 9 – OUTFLOW HYDROGRAPH FROM COAL-WASTE DAM AND LOCATION PLAN OF BUFFALO CREEK

500 acre-feet of impounded waters into Buffalo Creek valley, causing the most catastrophic flood in the state's history with the loss of 118 lives, 500 homes, and property damage exceeding $50 million. Observations were available on the approximate development sequence of the breach, the time required to empty the reservoir, indirect peak discharge measurements at four sites, approximate flood-peak travel times, and flood-peak elevations (Davies, et al., 1972). Cross-sections and estimates of the Manning roughness coefficients were taken from a report on routing dam-break floods by McQuivey and Keefer (1975).

The time of failure was estimated to be in the range of 5 minutes and the reservoir took only 15 minutes to empty according to eyewitnesses' reports. The following breach parameters were used: τ = 0.083 hours, b = 170 feet, z = 2.6 feet, h_{bm} = 0.0 feet, $h_f = h_d = h_o$ = 40.0 feet. Cross-sectional properties were specified for eight locations along the 15.7 mile reach from the coal-waste dam to below Man at the confluence of Buffalo Creek with the Guyandotte River as shown in Fig. 9. The downstream valley widened from the narrow width (approximately 100 ft) of Middle Fork to about 400-600 feet width of Buffalo Creek Valley. Minimum Δx (DXM) values were gradually increased from 0.2 mile near the dam to 0.4 mile near Man at the downstream boundary. The reservoir area-elevation values were obtained from Davies, et al., (1972).

The 15.7 mile reach was divided into two reaches; one was approximately 4 miles long, in which the very steep channel bottom slope (84 ft/mi) produced supercritical flows, and the second extended on downstream approximately 12 miles, with an average bottom slope of 40 ft/mi, in which subcritical flow prevailed. The computations were unstable when the supercritical reach was modeled using the same type of boundary conditions as used with subcritical flows. This computational problem was eliminated when the supercritical boundary condition, Eq. (62), was used.

The reservoir storage routing option was used to generate the outflow hydrograph shown in Fig. 9. The computations indicated the reservoir was drained of its contents in approximately 15 minutes, which agreed with the observed time to completely empty its contents. The indirect measurements of peak discharge at miles 1.1, 6.8, 12.1, and 15.7 downstream of the dam are shown in Fig. 10. Again, as in the Teton

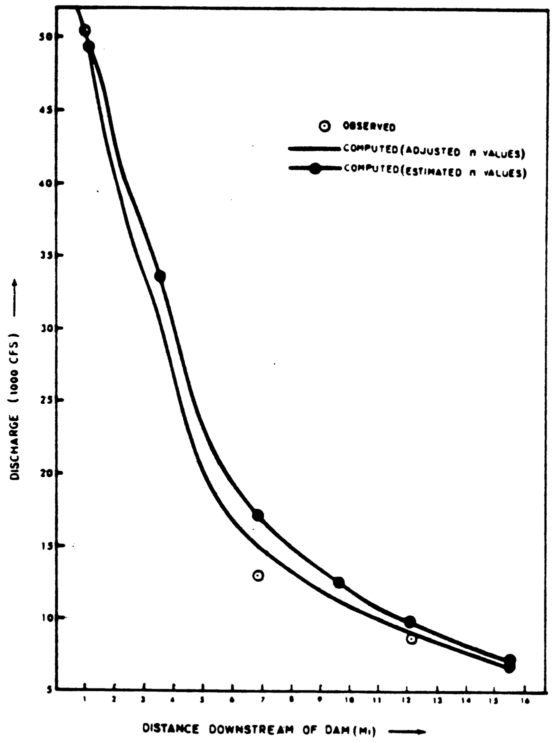

Fig. 10 – PROFILE OF PEAK DISCHARGE FROM BUFFALO CRK. FAILURE

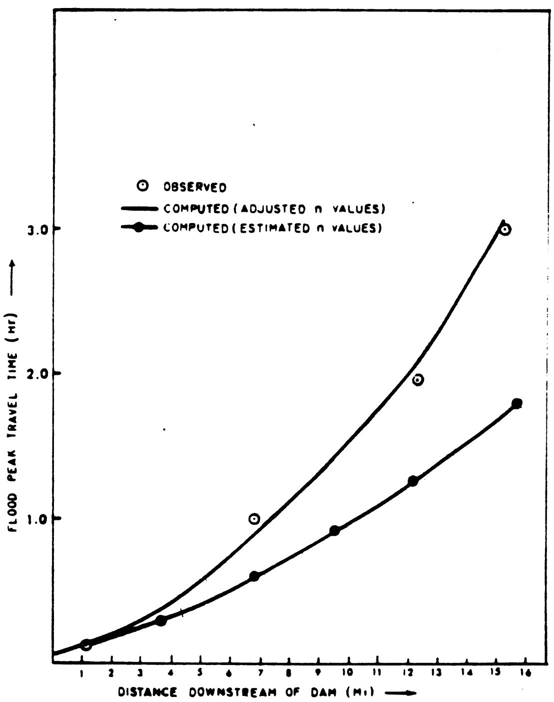

Fig. 11 – TRAVEL TIME OF FLOOD PEAK FROM BUFFALO CREEK FAILURE

Dam flood, the flood peak was greatly attenuated as it advanced downstream. Whereas the Teton flood was attenuated by a factor of 0.69 in the first 16 miles of which 11 miles included the wide, flat valley below the Teton Canyon, the Buffalo Creek flood was confined to a relatively narrow valley, but was attenuated by a factor of 0.88 in the same distance. The attenuation of the Buffalo Creek flood was due to the much smaller volume of its outflow hydrograph compared with that of the Teton flood.

In Fig. 10, the computed discharges agree favorably with the observed. There are two curves of the computed peak discharge in Fig. 10; one is associated with n values of 0.040. In the former, the n values are reresentative of field estimates, while the latter results from adjustments in the n values such that computed flood travel times compare favorably with the observed. (Comparison of computed flood travel times with the observed are shown in Fig. 11 for estimated n values and for the final adjusted n values.) It should be noted that the two computed curves in Fig. 10 are not significantly different, although the n values differ by a factor of 1.75. Again, as in the Teton application, the n values influence the time of travel much more than the peak discharge. The large adjusted n values appear to be appropriate for dam-break waves in the near vicinity of the breached dam where extremely high flow velocities uproot trees and transport considerable sediment and boulders (if present), and generally result in large energy losses.

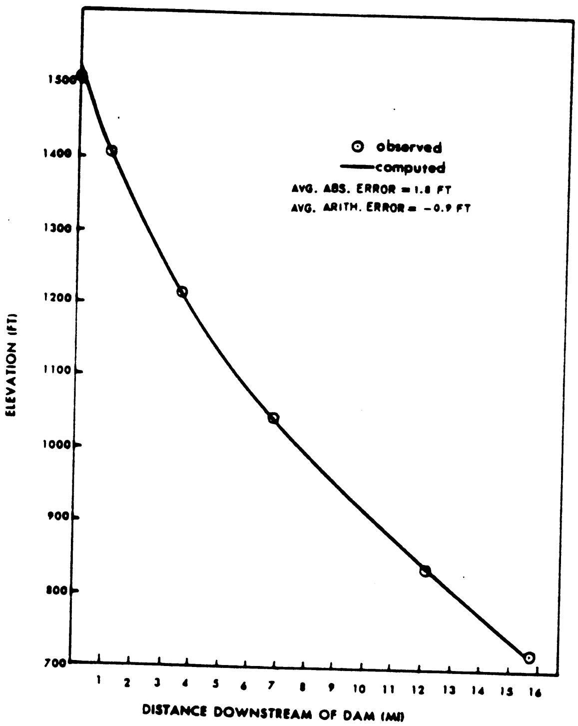

Fig. 12 – PROFILE OF PEAK FLOOD ELEVATION FROM BUFFALO CREEK FAILURE

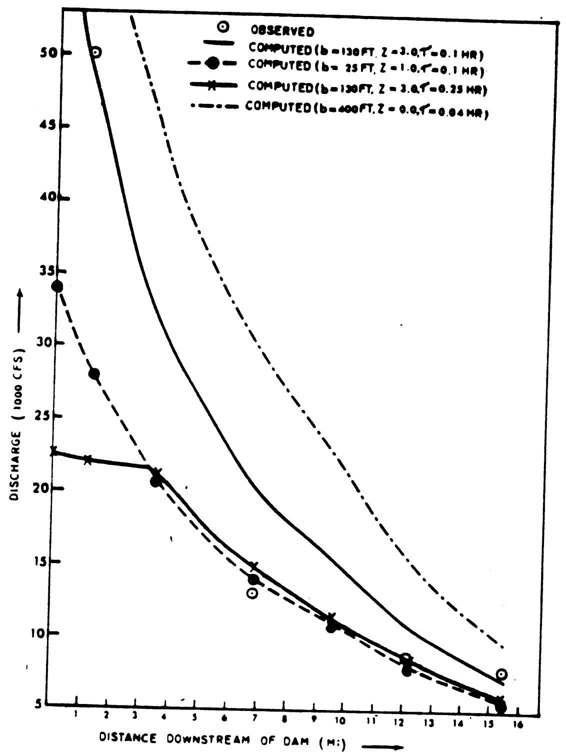

Fig. 13 – PROFILE OF PEAK DISCHARGE FROM BUFFALO CRK. FAILURE SHOWING SENSITIVITY OF VARIOUS INPUT PARAMETERS

A profile of the observed peak flood elevations downstream of the Buffalo Creek coal-waste dam is shown in Fig. 12, along with the computed elevations using adjusted n values. The average absolute error is 1.8 feet and the average arithmetic error is -0.9 foot.

Sensitivities of the computed downstream peak discharges to reasonable variations in the selection of breach parameters (τ, b, and z) are shown in Fig. 13. The resulting differences in the computed discharges diminish in the downstream direction. Like the Teton dam-break flood wave, errors in forecasting the breach are damped-out as the flood advances downstream.

A typical simulation of the Buffalo Creek flood involved 63 Δx reaches, 3.0 hours of prototype time, use of the reservoir storage routing option, and initial time step of 0.002 and 0.005 hour for the supercritical and subcritical downstream reaches, respectively. Computation time for a typical simulation run was 18 seconds (IBM 360/195).

5. FLOOD INUNDATION APPLICATIONS

The NWS DAMBRK model is suitable for the following two types of dam-break flood inundation applications: 1) pre-computation of flood peak elevations and travel times prior to a dam failure, and 2) real-time computation of the downstream flooding when a dam failure is imminent or has immediately occurred.

Pre-computations of dam failures enable the preparation of concise graphs or flash flood tables for use by those responsible for community preparedness downstream of critically located dams. The graphs provide information on flood peak elevations and travel times throughout the critical reach of the downstream valley. The variations in the precomputed values due to uncertainty in the breach parameters (τ and $\bar{b}$) can be included in the graph. Results obtained using a maximum probable estimate of $\bar{b}$ and a minimum probable estimate of τ would define the upper envelope of probable flood peak elevations and minimum travel times. Similarly, the use of a minimum probable estimated $\bar{b}$, would define the lower limit of the envelope of probable peak elevations and maximum travel times. In the precomputation mode, the forecaster can use as much of the capabilities of the DAMBRK model as time and data availability warrant.

Real-time computation is also possible in certain situations where the total response time for a dam-break flood warning exceeds a few hours. An abbreviated data input to DAMBRK can be used to quickly compute an approximate crest profile and arrival times. Computer coding forms have been prepared by the NWS Ft. Worth River Forecast Center with invariable parameters delineated and essential input data flagged. Using available topo maps and a minimum of information on the dam such as its height and storage volume, a forecast can be made within approximately 30 minutes.

In some cases it may be possible to make a revised forecast in real-time to update a pre-computed forecast when observations of the extent of the breach are made available to the forecaster. This would be valuable in refining the forecast for communities located far downstream where the possibility of flood inundation is questionable and the need for eventual evacuation can be more accurately defined by utilizing observations at the dam or actual flood elevations observed a few miles below the dam. The data set used to make the real-time update of the pre-computed forecast would have been retrieved from a data storage system and the critical parameters therein changed.

The DAMBRK model can also be used to route any specified flow through a river valley. In such applications of the model, the dam breach and reservoir routing data input and computational components are not used.

6. SUMMARY AND CONCLUSIONS

A dam-break flood forecasting model (DAMBRK) is described and applied to some actual dam-break flood waves. The model consists of a breach component which utilizes simple parameters to provide a temporal and geometrical description of the breach. A second component computes the reservoir outflow hydrograph resulting from the breach via a broad-crested weir-flow approximation, which includes effects of submergence from downstream tailwater depths and corrections for approach velocities. Also, the effects of storage depletion and upstream inflows on the computed outflow hydrograph are accounted for through storage routing within the reservoir. The third component consists of a dynamic routing technique for determining the modifications to the dam-break flood wave as it advances through the downstream valley, including its travel time and resulting water surface elevations. The dynamic routing component is based on a weighted, four-point non-linear finite difference solution of the one-dimensional equations of unsteady flow which allows variable time and distance steps to be used in the solution procedure. Provisions are included for routing supercritical flows as well as subcritical flows, and incorporating the effects of downstream obstructions such as road-bridge embankments and/or other dams.

Model data requirements are flexible, allowing minimal data input when it is not available while permitting extensive data to be used when appropriate.

The model was tested on the Teton Dam failure and the Buffalo Creek coal-waste dam collapse. Computed outflow volumes through the breaches coincided with the observed values in magnitude and timing. Observed peak discharges along the downstream valleys were satisfactorily reproduced by the model even though the flood waves were severely attenuated as they advanced downstream. The computed peak flood elevations were within an average of 1.5 ft and 1.8 ft of the observed maximum elevations for Teton and Buffalo Creek, respectively. Both the Teton and Buffalo Creek simulations indicated an important lack of sensitivity of downstream discharge to errors in the forecast of the breach size and timing. Such errors produced significant differences in the peak discharge in the vicinity of the dams; however, the differences were rapidly reduced as the waves advanced downstream. Computational requirements of the model are quite feasible; CPU time (IBM 360/195) was 0.005 second per hr per mile of prototype dimensions for the Teton Dam simulation, and 0.095 second per hr per mile for the Buffalo Creek simulation. The more rapidly rising Buffalo Creek wave (τ = 0.008hr as compared to Teton where τ = 1.25 hr) required smaller Δt and Δx computational steps; however, total computation times (Buffalo: 19 sec and Teton: 18 sec) were similar since the Buffalo Creek wave attenuated to insignificant values in a shorter distance downstream and in less time than the Teton flood wave.

Suggested ways for using the DAMBRK model in preparation of pre-computed flood information and in real-time forecasting were presented.

REFERENCES

Amein, M., and C. S. Fang, 1970: Implicit flood routing in natural channels. Journ. Hydraulic. Div., ASCE, 96, HY12, Dec., pp. 2481-2500.

Balloffet, A., 1977: Simulation of dam break flooding under normal and probable maximum flood conditions, Proceedings, Dam-Break Flood Modeling Workshop, U. S. Water Resources Council, Washington, D.C., pp. 384-401.

Balloffet, A., E. Cole, and A. F. Balloffet, 1974: Dam collapse wave in a river, Journ. Hydraul. Div., ASCE, 100, HY5, May, pp. 645-665.

Baltzer, R., and C. Lai, 1969: Computer simulation of unsteady flows in waterways. Journ. Hydraul. Div., ASCE, 94, HY4, July, pp. 1083-1117.

Brater, E., 1959: Hydraulics. Civil Engineering Handbook, edited by L. C. Urquhart, Sect. 4, McGraw-Hill Book Co., New York, pp. 4.44-4.60.

Brevard, J. A., and F. D. Theurer, 1979: Simplified dam-break routing procedure, Technical Release Number 66, U. S. Dept. of Agriculture, Soil Conservation Service, Engr. Div., 35 pp.

Brown, R. J., and D. C. Rogers, 1977: A simulation of the hydraulic events during and following the Teton Dam failure, Proceedings, Dam-Break Flood Modeling Workshop, U. S. Water Resources Council, Washington, D. C. pp.131-163.

Chaudhry, Y. M., and D. N. Contractor, 1973: Application of the implicit method to surges in open channels. Water Resour. Res., 9, No. 6, Dec., pp. 1605-1612.

Chen, C., and L. A. Druffel, 1977: Dam-break flood wave computation by method of characteristics and linearized implicit schemes, Proceedings, Dam-Break Flood Modeling Workshop, U. S. Water Resources Council, Washington, D. C., pp. 312-345.

Chow, V. T., 1959: Open-channel Hydraulics, McGraw-Hill Co., New York, pp. 476-481.

Cristofano, E. A., 1965: Method of computing rate for failure of earth fill dams. Bureau of Reclamation, Denver, Colo., April.

Cunge, J. A., 1975: Rapidly varying flow in power and pumping canals. Unsteady Flow in Open Channels, edited by K. Mahmood and V. Yevjevich, Vol. II, Chapt. 14, Water Resour. Pub., Ft. Collins, Colo., pp. 539-586.

Davidson, D. D., and B. L. McCartney, 1975; Water waves generated by landslides in reservoirs. Journ. Hydraul. Div., ASCE, 101, HY12, Dec., pp. 1489-1501.

Davies, W. E., J. F. Bailey, and D. B. Kelly, 1972: West Virginia's Buffalo Creek flood: a study of the hydrology and engineering geology. Geological Survey Circular 667, U. S. Geological Survey, 32 pp.

De Saint-Venant, Barre, 1871: Theory of unsteady water flow, with application to river floods and to propagation of tides in river channels. Acad. Sci. (Paris) Comptes rendus, 73, pp. 237-240.

Dressler, R. F., 1954: Comparison of theories and experiments for the hydraulic dam-break wave. Internat. Assoc. Sci. Pubs., 3, No. 38, pp. 319-328.

Fread, D. L., 1971: Discussion of implicit flood routing in natural channels. M. Amein and C. S. Fang. Journ. Hydraul. Div., ASCE, 97, HY7, July, pp.1156-1159.

Fread, D. L., and T. E. Harbaugh, 1973" Transient hydraulic simulation of breached earth dams, Journ. Hydraul. Div., ASCE, 99, HY1, Jan., pp 139-154.

Fread, D. L., 1974a: Numerical properties of implicit four-point finite difference equations of unsteady flow. NOAA Tech. Memo. NWS HYDRO-18, U. S. Dept of Commerce, NOAA, National Weather Service, 38 pp.

Fread, D. L., 1974b: Implicit dynamic routing of floods and surges in the Lower Mississippi. Presented at AGU Natl. Mtg., Wash., D. C., April, 26 pp.

Fread, D. L., 1975: Discussion of comparison of four numerical methods for flood routing, R. K. Price, Journ. Hydraul. Div., ASCE, 101, HY3, March, pp.565-567.

Fread, D. L., 1976: Flood routing in meandering rivers with flood plains, Proceedings, Rivers '76, Third Ann. Symp. of Waterways, Harbors and Coastal Eng. Div., ASCE, Vol. I, Aug., pp. 16-35.

Fread, D. L., 1977: The development and testing of a dam-break flood forecasting model, Proceedings, Dam-Break Flood Modeling Workshop, U. S. Water Resources Council, Washington, D. C., 1977, pp. 164-197.

Fread, D. L., 1978: NWS operational dynamic wave model, Verification of Mathematical and Physical Models in Hydraulic Engineering, Proceedings, 26th Annual Hydraulics Div. Specialty Conf., College Park, Md., Aug., pp.455-464.

Gundlach, D. L., and W. A. Thomas, 1977: Guidelines for calculating and routing a dam-break flood, Research Note No. 5, Corps of Engineers, U. S. Army, The Hydrologic Engr. Center, 50 pp.

Harris, G. W., and D. A. Wagner, 1967: Outflow from breached dams, Univ. of Utah.

Johnson, F. A., and P. Illes, 1976: A classification of dam failures, Water Power and Dam Construction, Dec., pp. 43-45.

Keefer, T. N., and R. K. Simons, 1977: Qualitative comparison of three dam-break routing models, Proceedings, Dam-Break Flood Modeling Workshop, U. S. Water Resources Council, Washington, D. C., pp.292-311.

Koutitas, C.G., 1977: Finite element approach to waves due to land-slides, Journ. Hydraul. Div., ASCE, 103, HY9, Sept., pp. 1021-1029.

Liggett, J., and J. A. Cunge, 1975: Numerical methods of solution of the unsteady flow equations. Unsteady Flow in Open Channels, edited by K. Mahmood and V. Yevjevich, Vol. I, Chapt. 4, Water Resour. Pub., Ft. Collins, Colo., pp. 89-182.

Martin, C. S., and J. J. Zovne, 1971: Finite-difference simulation of bore propagation. Journal. Hydraul. Div. ASCE, 97, HY7, July, pp. 993-1010.

McQuivey, R. S., and T. N. Keefer, 1976: Application of simple dam break routing model. Proceedings, 16th Congress, IAHR, Sao Paulo, Brazil, July 27-August 1, 1975, Vol. 2, pp. 315-324.

Middlebrooks, T. A., 1952: Earth-dam practice in the United States, Centennial Transactions, ASCE, Paper No. 2620, pp. 697-722.

Morris, H. M., and J. M. Wiggert, 1972: Applied Hydraulics in Engineering, The Ronald Press Co., New York, pp. 570-573.

Preissmann, A., 1961: Propagatin of translatory waves in channels and rivers. Paper presented at First Congress of French Assoc. for Computation, Grenoble, Sept. 14-16, Proceedings, AFCAL, pp. 433-442.

Price, J. T., G. W. Lowe, and J. M. Garrison, 1977: Unsteady flow modeling of dam-break waves, Proceedings, Dam-Break Flood Modeling Workshop, U. S. Water Resources Council, Washington, D. C., pp. 90-130.

Rajar, R., 1978: Mathematical Simulation of dam-break flow, Journ. Hydraul. Div., ASCE, 104, HY7, July, pp. 1011-1026.

Ray, H. A., L. C. Kjelstrom, E. G. Crosthwaite, and W. H. Low, 1976: The flood in southeastern Idaho from the Teton Dam failure of June 5, 1976. Unpublished open file report, U. S. Geological Survey, Boise, Idaho.

Re, R., 1946: A study of sudden water release from a body of water to canal by the graphical method. Houille Blanche (France), No. 3, pp. 181-187.

Ritter, A., 1892: The propagation of water waves. Ver. Deutsch Ingenieure Zeitschr. (Berlin), 36, Pt. 2, No. 33, pp. 947-954.

Sakkas, J. G., and T. Strelkoff, 1973: Dam break flood in a prismatic dry channel, Journ. Hydraul. Div., ASCE, 99, HY12, Dec., pp. 2195-2216.

Schocklitsch, A., 1917: On waves created by dam breaches. Akad. Wiss. (Vienna) Proc., 126, Pt. 2A, pp. 1489-1514.

Smith, R. H., 1978: Development of a dynamic flood routing model for small meandering rivers. Ph.D. dissertation, Univ. Missouri-Rolla, 159 pp.

Stoker, J. J., 1957: Water Waves, Inter-Science Pub., New York, pp. 333-341.

Strelkoff, T., 1970: Numerical solution of Saint-Venant equations. Journ. Hydraul. Div., ASCE, 96, HY1, Jan., pp. 223-252.

Su, S. T., and A. H. Barnes, 1970: Geometric and frictional effects on sudden releases. Journ. Hydraul. Div., ASCE, 96, HY11, Nov., pp. 2185-2200.

Terzidis, G., and T. Strelkoff, 1970: Computation of open channel surges and shocks. Journ. Hydraul. Div., ASCE, 96, HY12, Dec., pp. 2581-2610.

Thomas, W. A., 1977: Calculating and routing of the Teton dam-break flood, Proceedings, Dam-Break Flood Modeling Workshop, U. S. Water Resources Council, Washington, D. C., pp. 198-227.

U. S. Army Corps of Engineers, 1960: Floods resulting from suddenly breached dams--conditions of minimum resistance, hydraulic model investigation. Misc. Paper 2-374, Report 1, WES, Feb., 176 pp.

U. S. Army Corps of Engineers, 1961: Floods resulting from suddenly breached dams--conditions of high resistance, hydraulic model investigation. Misc. Paper 2-374, Report 2, WES, Nov., 121 pp.

U. S. Army Corps of Engineers, 1975, National Program of Inspection of Dams, Bol. I-4, Dept. of the Army, Office of Chief of Engineers, Washington, D. C.

U. S. Dept. Transportation/Federal Highway Administration, 1978: Hydraulics of Bridge Waterways, Hydraulic Design Series No. 1, Washington, D. C., pp. 45-46.

Venard, J. K., 1954: Elementary Fluid Mechanics, John Wiley and Sons, New York, pp. 312-325.

APPENDIX A

INPUT DATA STRUCTURE FOR DAM-BREAK (DAMBRK): 07/18/84

Input card group no.

(1) MDAM, MRVR, MNAME - 20 A 4 Format

MDAM	Name of dam (col. 1-20).
MRVR	Name of reservoir (col. 21-40).
MNAME	Agency name (col. 41-60).

MESAGE - 20 A 4 Format

MESAGE	Agency address--street, room (col. 1-40). Agency Address--city, state, zip code (col. 41-72).

(2) KKN, KUI, MULDAM, KDMP, ITEH, NPRT, KFLP, KSL - 8 I 10 Format

KKN — Parameter which is associated with KSUPC on card (16). If KSUPC=0, KKN=1; if KSUPC=1, KKN should be given a value of 1 if the downstream channel valley below the dam is entirely supercritical flow or KKN should be given a value of 2 if the downstream reach is divided into two reaches (an upstream reach having supercritical flow and a downstream reach having subcritical flow). If KKN=9, a hydrograph is read in and then routed through the downstream valley.

KUI — Parameter used to select type of reservoir routing for determining outflow hydrograph; if KUI=0, storage routing is used; if KUI=1, dynamic routing is used.

MULDAM — Parameter used to select option for routing through multiple reservoirs sequentially located downstream of first dam. If one or more dams are located downstream of first dam, MULDAM=1, if no dams are downstream of first dam, then MULDAM=0. Any number of downstream sequentially located dams may be simulated by letting KKN=1 + no. of downstream dams.

KDMP — Parameter for printing; users outside of the National Weather Service set KDMP=3. KDMP=0, print only title page; KDMP=1, title page, abstract, variable descriptions; KDMP=2, same as KDMP=1 plus input data; KDMP=3, title page plus input data; KDMP=4, same as KDMP=2, then stop; if KDMP=5, IOPUT on card (4) allowing selective printout of computations is read-in and KDMP is reset to 3.

ITEH	Parameter denoting number of hydrograph ordinates of inflow hydrograph to reservoir; maximum value of 50 is allowed; if ITEH=0, the inflow hydrograph is generated via a mathematical function.
NPRT	Parameter to control print output for JNK=9, NPRT is the total number of cross-sections at which hydraulic information is printed-out during dynamic routing; if NPRT=0, the program uses a variable NPRT computed by the program and prints-out hydraulic information at NPRT intervals of cross-sections along the routing reach.
KFLP	Parameter denoting the use of the special flood-plain routing feature; if KFLP=0, the special flood-plain feature is <u>not</u> used; if KFLP=1, the special flood-plain routing is used.
KSL	Parameter denoting simulation of landslide; if KSL=0, <u>no</u> landslide; if KSL=1, a landslide occurring along one bank of the reservoir is simulated; if KSL=2, the landslide occurs along both banks of reservoir.

(3) NPT(K) - 8 I 10 Format

NPT(K)	Sequential number of cross-section at which hydraulic information is printed-out; this card is omitted if NPRT=0; K index goes from 1 to NPRT where NPRT $\leq$ 30.

(4) IOPUT(K) - 10 I 1, 2 I 2 Format

IOPUT(K)	Optional print parameter that may override the JNK parameter, (card 16). K index goes from 1 to 12. If IOPUT(K)=0, allow the output to be printed; if IOPUT(K)=1, suppress the output. The following output can be controlled:

Col	
1	Slope profile plot
2	Summary tables of input x.s. and reaches
3	Initial conditions table - flow and "L" tables (reversed)
4	Initial conditions table - backwater elevation table (forward)
5	Dynamic routing - at upstream and downstream boundaries
6	Dynamic routing - at each multiple dam site (similar to depletion table)
7	Summary plots - peak elevation, discharge, time to peak, and time to flood elevation
8	Arrays for selected hydrograph plots
9	List of input cross-sectional information
10	Reservoir depletion table

Col

11-12 This value reperesents the time at which printing of output will commence. All output will be suppressed until this time is reach.

13-14 The interval at which the output will be printed.

Note: This information can only be controlled if the JNK parameter allowed it to be printed originally.

(5) IDAM(K) - 8 I 10 Format

IDAM(K) Number of cross-section coincident with the upstream face of each dam; K index goes from 1 to MULDAM. This parameter is only read-in when the simultaneous computation of the complete system is desired (see note on page A-21 for further information on the use of this computational option).

(6) SA(K) - 8 F 10.0 Format

SA(K) Surface area (acres) or volume (acre-ft) of reservoir at elevation HSA(K). If KUI=1 and KKN≠1 or KKN=9, omit card (6). Maximum of 8 values allowed.

(7) HSA(K) - 8 F 10.0 Format

HSA(K) Elevation (ft) at which reservoir surface area SA(K) is defined; elevation is referenced to a datum plane corresponding to mean sea level (m.s.l.). If KUI=1 and KKN≠1 or KKN=9, omit card (7). Elevations start at highest and proceed to lowest. Maximum of 8 values allowed. Lowest elevation must be YBMIN as defined on card (8).

(8) RLM, YO, Z, YBMIN, BB, TFH, DATUM, VOL - 8 F 10.0 Format

RLM	Length (mi) of reservoir.
YO	Elevation (ft) of water surface in reservoir when computation commences; elevation is referenced to m.s.l. datum.
Z	Side slope (1:vertical to z:horizontal) of breach.
YBMIN	Lowest elevation (ft) that bottom of breach reaches; elevation is referenced to m.s.l. datum.

BB	Width (ft) of base of breach.
TFH	Time (hr) from beginning of breach formation until it reached its maximum size.
DATUM	Elevation (m.s.l.) of bottom of dam.
VOL	Parameter indicating if SA(K) is surface area (acres) or volume (acre-ft); if VOL=0.0, SA(K) is acres; if VOL=1.0, SA(K) is acre-ft.

(9) HF, HD, HSP, HGT, CS, CG, CDO, QT - 8 F 10.0 Format

HF	Elevation (ft) of water when failure of dam commences; elevation is referenced to m.s.l. datum; if HF is less than HD, the breach is formed by "piping."
HD	Elevation (ft) of top of dam; elevation is referenced to m.s.l. datum.
HSP	Elevation (ft) of uncontrolled spillway crest; elevation is referenced to m.s.l. datum.
HGT	Elevation (ft) of center of gate openings; elevation is referenced to m.s.l. datum.
CS	Discharge coefficient for uncontrolled spillway; it is equal to the coefficient of discharge (2.6-3.2) times the length (ft) of the spillway.
CG	Discharge coefficient for gate flow; it is equal to the coefficient of discharge (0.60-0.80) times the area of gates.
CDO	Discharge coefficient for uncontrolled weir flow over the top of the dam; it is equal to the coefficient of discharge (2.6-3.2) times the length of the dam crest (ft) less the length of the uncontrolled spillway and gates.
QT	Discharge (cfs) through turbines; this flow is assumed constant from start of computations until the dam is completely breached; thereafter, QT is assumed to be zero. QT may also be considered leaking or constant spillway flow.

<u>Note:</u> Omit cards (8) and (9) if KKN=9.

(10) QSPILL(K,L) - 8 F 10.0 Format

QSPILL(K,L)	Flow (cfs) of spillway or gate rating curve; K goes from 1 to maximum of 8; L goes from 1 to MULDAM (card (2)) which may be a maximum of 10; if MULDAM=0, L goes from 1 to 1.

(11) HEAD(K,L) - 8 F 10.0 Format

HEAD(K,L) Head (ft) above spillway crest or gate center; head is associated with spillway flow or gate flow in rating curve; K goes from 1 to maximum of 8; L goes from 1 to MULDAM.

Note: Repeat cards 10-11 as L index goes from 1 to MULDAM. If MULDAM=0, L index goes from 1 to 1.

Note: Cards (10) and (11) are read-in only if either HSP is non-zero and CS is zero, or HGT is non-zero and CG is zero. This option allows a rating curve to be used for either the uncontrolled spillway or submerged gate rather than an equation for each using a constant discharge coefficient as in Eq. (17).

(12) DHF, TEH - 2 F 10.0 Format

DHF Interval (hr) between QI(K) input hydrograph ordinates; enter 0.0 if intervals are not equal.

TEH Time (hrs) from beginning of routing until routing is terminated.

(13) QO, RHO, GAMA, TPG - 4 F 10.0 Format

QO Initial steady discharge (cfs).

RHO Ratio of peak flow to initial flow of inflow hydrograph.

GAMA Ratio of time from initial steady flow to center of gravity of inflow hydrograph to time to peak of inflow hydrograph.

TPG Time from initial flow to peak flow of inflow (hr).

Note: Omit card 13 if ITEH (card 2) is nonzero.
If card 13 is included, then omit cards (14) and (15).

(14) QI(K) - 8 F 10.0 Format

QI(K) Inflow (cfs) at upstream end of reservoir for each interval of time during the failure and until time TEH is reached; K goes from 1 to ITEH which can assume a maximum value of 50; if ITEH=0, omit this card.

(15) TI(K) - 8 F 10.0 Format

TI(K) — Time associated with QI(K) inflows; if DHF (card 12) is non-zero, or if ITEH (card 2) is equal to zero, omit this card, K goes from 1 to ITEH.

(16) NS, NCS, NTT, JNK, KSA, KSUPC, LQ, KCG - 8 I 10 Format

NS — Number of cross-sections used to describe the channel and valley downstream of dam; first cross-section should be immediately downstream of dam; last cross-section should be at farthest point downstream of dam where flood information is desired; other cross-sections can be located as desired by user; maximum of 90 and minimum of 2 cross-sections can be used to describe the downstream channel valley.

NCS — Maximum numer of top widths used to describe a cross-section.

NTT — Total number of cross-sections at which discharge hydrographs will be plotted; maximum number is limited to 6. The location of the cross-sections at which plots are provided is specified by the parameter NT(K), which is on card (17). If NTT=0, no plots are provided. If NTT=a negative value between 1 and 6, the profile plots are suppressed.

JNK — Parameter to specify the type of output other than plots which will be provided; if JNK=0, a minimum of output is provided--this includes all input data and hydrograph plots; if NTT=0, no hydrographs or other output printed; if JNK=1, reservoir depletion table printed, profile of downstream crests and times, and designated hydrographs; if JNK=4, additional information is printed at each time step for debugging; if JNK=9, information is printed for debugging.

KSA — Parameter to enable downstream channel-valley cross-sections to be specified by a surface area vs. elevation table similar to the SA(K) and HSA(K) values described above; if KSA=1, downstream channel-valley cross-sections will be described by input data consisting of a single table of surface area vs. elevations as indicated for cards (24) and (25); if KSA=0, this option is not used.
Also, a parameter to indicate type of cross section smoothing. If KSA<0, then smoothing of cross sections will be automatically performed. Type of smoothing is specified on card (18).

KSUPC	Parameter to indicate if flow is supercritical. If KSUPC=0, flow through entire downstream channel-valley reach is subcritical and no special treatment is required; if KSUPC=1, the flow is known to be supercritical in either an upstream portion of the downstream channel-valley or throughout the entire downstream reach. When flow is supercritical, special computational procedures are used within the program. If only the upstream portion of the reach has supercritical flow, two sets of downstream channel-valley inputs commencing with card no. (16) are read in.
LQ	Parameter denoting the total number of lateral inflow hydrographs along the downstream channel-valley; a maximum of 10 hydrographs, each with 50 ordinates, are allowed.
KCG	Number of ordinates in spillway gate control curve of gate coefficient (CGCG) vs. time (TCG) described on cards (43) and (46). If KCG is negative, it is the total number of floodplain compartments. Maximum of 16 allowed.

Note: For debugging, JNK=4 or 9 is preferred.

(17) NT(K) - 6 I 10 Format

NT(K)	Number of cross-section (1 through NS) at which hydrograph plots are desired; K goes from 1 to NTT: if NTT=0, card no. (17) is omitted.

(18) SMF, NTSM, NSMR - F10.2, 2 I 10

SMF	Smoothing factor, $0.5 \leq \text{SMF} \leq 0.9$.
NTSM	Parameter indicating type of smoothing. If NTSM=1, smoothing of widths along x-axis; if NTSM=2, smoothing of widths in vertical where maximum width/ft change is |KSA|*50; if NTSM=3, smoothing of elevations along x-axis; NTSM=4, type 1 and type 2 smoothing; if NTSM=5, type 1, 2, and 3 smoothing.
NSMR	Number of separate smoothing reaches within the total routing reach.

(19) NUSM(K), NDSM(K) - 2 I 10

NUSM(K)	Upstream cross section number of K^{th} smoothing reach.
NDSM(K)	Downstream cross section number of K^{th} smoothing reach.

Note: Card (19) is read-in for each K^{th} smoothing reach as K goes from 1 to NSMR.

Note: Omit cards 18 and 19 if KSA $\geq$ 0 (card 16)

(20) XS(I), FSTG(I), XSL(I), XSR(I) - 4 F 10.0 Format

XS(I) — Location (mi) of cross-sections used to describe downstream channel-valley; mileage must increase in the downstream direction from dam. If KFLP=1 (card (2)), XS(I) is mileage measured along center of channel.

FSTG(I) — Elevation (m.s.l.) at which flooding commences; may be left blank.

XSL(I) — If KFLP=0, leave blank; if KFLP=1, XSL(I) is the mileage (location) of the I^{th} cross-section along the left (looking upstream) flood-plain.

XSR(I) — If KFLP=0, leave blank; if KFLP=1, XSR(I) is the mileage (location) of the I^{th} cross-section along the right flood-plain.

(21) HS(K,I) - 8 F 10.0 Format

HS(K,I) — Elevation (ft), referenced to m.s.l. datum, corresponding to each top width (BS(K,I)) on card (22) used to describe cross-section; K goes from 1 to NCS; NCS values of HS(K,I) are punched on a single card. NCS is limited to a maximum of 8. Start with lowest HS and proceed to highest value of HS.

(22) BS(K,I) - 8 F 10.0 Format

BS(K,I) — Top width (ft) of active flow portion of channel-valley cross-section corresponding to each elevation HS(K,I); K goes from 1 to NCS; NCS values of BS(K,I) are punched on a single card; NCS is limited to maximum of 8. This card is omitted if KSA=1.

(23) BSL(K,I) - 8 F 10.0 Format

BSL(K,I) — Top width (ft) of active flow portion of left flood-plain corresponding to each elevation HS(K,I); K goes from 1 to NCS; NCS values of BSL(K,I) are punched on a single card; NCS is limited to a maximum of 8. This card is omitted if KFLP=0 (card (2)).

(24) BSR(K,I) - 8 F 10.0 Format

BSR(K,I) Top width (ft) of active flow portion of right floodplain corresponding to each elevation HS(K,I). This card is omitted if KFLP=0.

(25) BSS(K,I) - 8 F 10.0 Format

BSS(K,I) Top width (ft) of off-channel storage portion of channel-valley cross-section corresponding to each elevation HS(K,I); K goes from 1 to NCS; NCS values of BSS(K,I) are punched on a single card; NCS is limited to maximum of 8; this card is omitted if KSA=1 (card (16)).

(26) DSA(K,I) - 8 F 10.0 Format

DSA(K,I) Surface area (acres) of active flow portion of downstream channel-valley cross-section corresponding to each elevation HS(K,I); K goes from 1 to NCS; NCS values of DSA(K,I) are punched on a single card; NCS is limited to maximum of 8; this card is omitted if KSA < 0.

(27) SSA(K,I) - 8 F 10.0 Format

SSA(K,I) Surface area (acres) of off-channel storage portion of channel valley cross-section corresponding to each elevation HS(K,I); K goes from 1 to NCS; NCS values of SSA(K,I) are punched on a single card; NCS is limited to maximum of 8; this card is omitted if KSA=0.

Note: Cards (20)-(25) are repeated for each cross-section as in the index I goes from 1 to NS.
When KSA=1, the cards are read-in as follows: (20), (21), (26), (27), (20), (21); this option is limited to the case of NS=2.

(28) CM(K,I) - 8 F 10.0 Format

CM(K,I) Manning n for channel corresponding to each elevation HS(K,I); K goes from 1 to NCS: NCS values of CM(K,I) are punched on a single card; NCS is limited to maximum of 8; the Manning n represents the roughness enountered by the flow through the reach bounded by cross-sections at locations I and I+1.

(29) CML(K,I) - 8 F 10.0 Format

CML(K,I) Manning n for left flood-plain corresponding to each elevation HS(K,I); K goes from 1 to NCS; NCS values of CM(K,I) are punched on a single card; NCS is limited to a maximum of 8. This card is omitted if KFLP=0 (card 2).

(30) CMR(K,I) - 8 F 10.0 Format

CMR(K,I) Manning n for right flood-plain corresponding to each elevation HS(K,I). This card is omitted if KFLP=0.

Note: Cards (28, 29, 30) are repeated for (NS-1) reaches.

(31) DXM(I) - 8 F 10.0 Format

DXM(I) Minimum Δx distance (mi) between cross-sections used in the computations. If DXM(I) is less than the distance between two adjacent cross-sections among the NS cross-sections read in, then intermediate cross-sections are created within the program via an interpolation procedure. (NS-1) values of DXM(I) are punched on one or more cards (8 values to a card); maximum no. of DXM(I) values is limited to 89; values assigned to DXM(I) should not result in more than 200 cross-sections produced by the interpolation procedure. (DXM values should be determined by the relationship C times Δt, where C is the approximate speed of the flood wave.)

(32) FKC(I) - 8 F 10.0 Format

FKC(I) Contraction-expansion coefficient; contraction values vary from 0.1 to 0.3, expansion values vary from -0.5 to -1.0; if contraction-expansion effects are negligible, enter 0.0 for FKC(I); (NS-1) values of FKC(I) are punched on one or more cards (8 values to a card); maximum no. of FKC(I) values is limited to 89.

(33) QMAXD, QLL, DTHM, YDN, SOM, FII, EPSY, TFI - 8 F 10.0 Format

QMAXD Estimated maximum discharge (cfs) at downstream extremity of channel-valley reach; can be read in as 0.0 for initial run; subsequent runs can have a value of QMAXD as determined by the routing computations during the initial run. Only required when QLL is non-zero.

QLL Maximum lateral outflow (cfs/ft) producing the volume losses experienced by the passage of the dam-break flood wave through the downstream valley; QLL has a negative sign and is computed by Eq. (63) in paper.

DTHM Initial Δt time step size (hr); if 0.0 is read in, the value of DTHM is computed by the program; if DTHM<0.0, DTHM represents the divisor MDT for determining the time step (DTH=TFH/MDT) and DTHM is reset to zero. See note on page A-23.

YDN Initial elevation of water surface at downstream end of routing reach; if channel control exists at this location, enter 0.0; YDN is non-zero if a dam or other control structure exists at the downstream end of the routing reach; if YDN=0.25, a single value rating curve of water surface elevation (m.s.l.) vs. discharge exists at downstream end; if YDN=0.5, critical flow such as waterfall exists at downstream end; if YDN=0.75, a specified water surface elevation (m.s.l.) such as a tide exists at the downstream end; if YDN=1.0, channel control exists at downstream end, but this signals the program that initial water surface elevations will be read-in at the NS cross-sections via card (48).

SOM Slope of downstream channel (ft/mi) for first mile below dam.

FII Theta (Θ) weighting factor in finite difference solution; if left blank, a value of 0.60 is used in program; if 0.5 is used, Θ is set internally to 0.60 and the model is capable of allowing negative flows to occur; if 0.51 is used, Θ is set internally to 0.60 and the model routing is done by the diffusion method instead of dynamic routing.

EPSY Convergence criterion for stage (ft) in Newton-Raphson iterative solution of finite difference unsteady flow equations; varies from .01 to .1 ft; if left blank, program use 0.01 ft. Also, can be used to specify the exponent m used in Eq. 65 in the paper; if EPSY<0.50, m=4; if EPSY>0.5, m=EPSY and EPSY is automatically set to 0.01.

TFI Time (hr) when time step changes from DTHM to TFH/MDT. See time step note on page A-23.

(34) NPLD - I 10

NPLD — Number of last floodplain compartment on same side of river where first floodplain compartment (FPC) is located; if no flow is transferred from one FPC to an adjacent FPC, let NPLD=0. Omit this card if KCG$\geq$0.

(35) NPXI(K), NQLP(K), PWELV(K), PCWR(K), PEO(K), QMINP(K) - 2 I 10, 4 F 10.0

NPXI(K) — Number of cross section immediately upstream of Δx reach where inflow to K^{th} FPC occurs.

NQLP(K) — Parameter indicating if pump discharge within the K^{th} FPC will be specified by a discharge hydrograph; 0 if no, 1 if yes.

PWELV(K) — Average elevation (ft. msl) of crest of weir (levee) along Δx reach where inflow to K^{th} FPC occurs.

PCWR(K) — Coefficient of discharge for weir flow along Δx reach where inflow to K^{th} FPC occurs; ranges in value from 2.6 to 3.2.

PEO(K) — Initial elevation (ft. msl) of water surface in K^{th} FPC at time = 0.

QMINP(K) — Minimum discharge (cfs) of total number of pumps in K^{th} FPC at all times.

(36) PSA(I,K) - 8 F 10.0

PSA(I,K) — Total volume (acre-ft) of K^{th} FPC below each elevation (PEL(I,K)); I index goes from 1 to 8.

(37) PEL(I,K) - 8 F 10.0

PEL(I,K) — Elevation (ft. msl) associated with each volume (PSA(I,K); elevations start at the lowest and proceed to the highest; I index goes from 1 to 8; last specified elevation should be greater than any expected water elevation within the FPC.

(38) QPU(I,K) - 8 F 10.0

QPU(I,K) — Inflow (cfs) to K^{th} FPC other than that transmitted over the weir (levee) from the main river; I index goes from 1 to ITEH (card no. 2).

(39) QLP(I,K) - 8 F 10.0

QLP(I,K) Specified total pump discharge (cfs) for K^{th} FPC; I index goes from 1 to ITEH (card no. 2); omit this card if NQLP(K)=0.

(40) COFF(I,K) - 8 F 10.0

COFF(I,K) Coefficient of discharge for flow over levee separating the K^{th} and K^{th}+1 FPC; coefficient is product of the broad-crested weir coefficient (2.6 to 3.2) and the length (ft) of the weir crest; the coefficient varies with elevation (HCFF(I,K)); I index goes from 1 to 8; omit this card if NPLD=0.

(41) HCFF(I,K) - 8 F 10.0

HCFF(I,K) Elevation (ft. msl) associated with the discharge coefficients (COFF(I,K)); elevations start at the lowest point along the levee crest and proceed upward; I index goes from 1 to 8; omit this card if NPLD=0.

Note Omit card no. 34 to 45 if KCG$\geq$0; otherwise repeat card no. 33 to 41 as K index goes from 1 to ABS(KCG).

(42) NPM - I 10

NPM Total number of pumps in all the FPC.

Note> Omit card no. 43 to 45 if NPM=0.

(43) IPMPL(L), NXPO(L), PEMN(L), PEMX(L) - 2 I 10, 2 F 10.0

IPMPL(L) Number of the K^{th} FPC in which the L^{th} pump is located.

NXPO(L) Number of the cross section immediately upstream of Δx reach where the L^{th} pump discharges into main river.

PEMN(L) Elevation (ft. msl) of water in K^{th} FPC when L^{th} pump starts pumping.

PEMX(L) Elevation (ft. msl) of water in K^{th} FPC when Lth pump stops pumping.

(44) DHP(I,L) - 8 F 10.0

DHP(I,L) Head (ft) associated with L^{th} pump rating curve; I index goes from 1 to 8; head starts at smallest and proceeds to greatest; negative head may be specified. Omit this card if NQLP(K)=0.

(45) OP(I,L) - 8 F 10.0

OP(I,L) Pump discharge (cfs) associated with L^{th} pump rating curve; I index goes from 1 to 8; each value is associated with its corresponding DHP(I,L) value. Omit this card if NQLP(K)=0.

Note Repeat card no. 43 to 45 as L index goes from 1 to NPM.

(46) LQX(K) - 8 I 10 Format

LQX(K) Number of cross-section immediately upstream of lateral inflow/outflow; K goes from 1 to LQ (card (16)). If LQX(K) is specified as a negative number, this indicates that the reach may have outflow via broad-crested weir flow.

(47) QL(L,K) - 8 F 10.0 Format

QL(L,K) Lateral inflow (cfs) for k^{th} lateral inflow point; L index goes from 1 to ITEH (card (2)); ordinates of lateral inflow hydrograph have same times as those of reservoir inflow hydrograph (QI(L)) on card (14)); K index goes from 1 to LQ.

If LQX(K) is negative, two values only are specified on card (47) according to a 2 F 10.2 format. The first (WELV(K)) is the crest elevation (msl) at which overflow occurs (this represents the average crest elevation along the reach). The second (CWR(K)) is the discharge coefficient ranging in value from 2.6 to 3.2 with 3.0 a most common value.

Note: Omit cards (46) and (47) if LQ=0 (on card no. 16).

(48) YD(I) - 8 F 10.0 Format

YD(I) Initial water surface elevations (m.s.l.) along routing reach; this is used only if YDN=1.0; if YDN≠1.0, omit this card and program computes the initial water surface elevations.

(49) RH(K) - 8 F 10.0 Format

RH(K) Elevation (m.s.l.) points on single value rating curve for downstream boundary, read in only if YDN (card no. 33) = 0.25; K index goes from 1 to maximum of 8.

(50) RQ(K) - 8 F 10.0 Format

RQ(K) Discharge (cfs) associated with elevation points on single value rating curve for downstream boundary, read in only if YDN=0.25.

(51) STN(K) - 8 F 10.0 Format

STN(K) Specified water surface elevation (m.s.l.) at downstream boundary such as a tide; K goes from 1 to ITEH, read in only if YDN=0.75.

(52) TTN(K) - 8 F 10.0 Format

TTN(K) Time (hrs) associated with STN(K); K goes from 1 to ITEH, read in only if YDN=0.75.

(53) NSLI - I 10 Format

NSLI Total no. of cross-sections (read-in) where landslide occurs; maximum no. allowed is 6; also maximum total cross-sections (including interpolated ones created by DXM values on card (31)) is limited to 31; omit if KSL=0 (card (2)).

(54) NXSLI(K), TSL, HSL(K), HSM(K), HSU(K), THKSL(K), ALPHA, POR - I 10, 7 F 10.2 Format

NXSLI(K)	Sequential number of cross-section where landslide occurs; K index goes from 1 to NSLI.
TSL	Time of duration for landslide (usually in the range of 15 seconds to a few minutes); unit must be in hrs.
HSL(K)	Elevation (ft above m.s.l.) of lowest portion of landslide mass; K goes from 1 to NSLI.
HSM(K)	Elevation (ft above m.s.l.) of middle portion of landslide mass--at this elevation, the landslide mass has the greatest thickness into the bank; K goes from 1 to NSLI.
HSU(K)	Elevation (ft above m.s.l.) of highest portion of landslide mass, K goes from 1 to NSLI.
THKSL(K)	Greatest thickness (depth into the bank) in ft of the landslide mass at elevation HSM(K); K goes from 1 to NSLI.
ALPHA	Angle of repose that deposited material from the landslide assumes in the bottom of the reservoir, in degrees.
POR	Porosity of landslide material, decimal fraction.

Note: Omit cards (53) and (54) if KSL=0.

Note: Card (54) is repeated for each K as it goes from 1 to NSLI.

(55) ICG(K) - 8 I 10 Format

ICG(K)	Parameter indicating if a dam has time-dependent gate flow; if yes, ICG(K)=1; if no, ICG(K)=0; K goes from 1 to M, where M=MULDAM if MULDAM≥1 and M=1 if MULDAM=0.

(56) CGCG(L,K) - 8 F 10.0 Format

CGCG(L,K)	Spillway gate coefficient equal to area of gates (opened at time TCG(L,K)) x coefficient of discharge; L goes from 1 to KCG (see card 16); and K goes from 1 to the total number of dams having time-dependent gate control.

(57) GBL(L,K) - 8 F 10.0 Format

GBL(L,K) Distance (ft) from bottom of gate to gate sill (HGT-card(9)); This distance is time dependent and is associated with the time array TCG(L,K); L and K index are same as described on card (56).

(58) TCG(L,K) - 8 F 10.0 Format

TCG(L,K) Time (hrs) associated with CGCG(L,K); L goes from 1 to KCG; and K goes from 1 to the total number of dams having time-dependent gate control.

Note: Omit cards (55), (56, (57), and (58) if KCG=0 (on card no. 16).

(59) Z, YBMIN, BB, TFH - 4 F 10.0 Format

Z	Side slope (1:vertical to z:horizontal) of breach of downstream dam.
YBMIN	Lowest elevation (ft) that bottom of breach reaches; elevation is referenced to m.s.l. datum.
BB	Width (ft) of base of breach of downstream dam.
TFH	Time (hr) from beginning of breach formation of downstream dam until it reaches its maximum size.

(60) HF, HD, HSP, HGT, CS, CG, CDO, QT - 8 F 10.0 Format

HF	Elevation (ft) of water when failure of downstream dam commences; elevation is referenced to m.s.l. datum.
HD	Elevation (ft) of top of downstream dam; elevation is referenced to m.s.l. datum.
HSP	Elevation (ft) of uncontrolled spillway crest; elevation is referenced to m.s.l. datum.
HGT	Elevation (ft) of center of gate openings; elevation is referenced to m.s.l. datum.
CS	Discharge coefficient for uncontrolled spillway; it is equal to the coefficient of discharge (2.6-3.2) times the length (ft) of the spillway.
CG	Discharge coefficient for gate flow; it is equal to the coefficient of discharge (0.10-0.80) times the area of gates.
CDO	Discharge coefficient for uncontrolled weir flow over the top of the downstream dam; it is equal to the coefficient of discharge (2.6-3.2) times the length of the downstream dam crest (ft) less the length of the uncontrolled spillway and gates.

QT — Discharges (cfs) through turbines; this flow is assumed constant from start of computations until the downstream dam is completely breached; thereafter QT is assumed to be zero.

(61) QSPILL(K,1) - 8 F 10.0 Format

QSPILL(K,1) — Flow (cfs) of spillway or gate rating curve; k goes from 1 to maximum of 8.

(62) HEAD(K,1) - 8 F 10.0 Format

HEAD(K,1) — Head (ft) above spillway crest or gate center; head is associated with spillway flow or gate flow in rating curve.

Note: Cards (61) and (62) are read-in only if either HSP is non-zero and CS is zero or HGT is non-zero and CG is zero. This option allows a rating curve to be used for either the uncontrolled spillway or submerged gate rather than an equation for each using a constant discharge coefficient as in Eq. (17).

(63) UPSH, SOM, CMN - 3 F 10.0 Format

UPSH — Dummy variable, leave blank.
SOM — Slope of downstream channel (ft/mi) for first few miles below dam.
CMN — Average Manning's n for downstream channel for first few miles below dam.

Note: Cards (59-63) are omitted if KUI=0 and MULDAM=0 or if KKN=9.

Note: If KUI=1 and dynamic routing is used for the reservoir routing procedure, cards (6) and (7) are omitted and cards (8)-(58) and (51) apply to the reservoir characteristics. Then, cards (16)-(58) are read in again; this time they apply to the downstream channel and valley.

Note: If KKN=9, only a downstream routing is used to route a read-in hydrograph (cards (12)-(15)). Also, cards (16)-(25) and (28)-(58) are required.

Note: The program has the capability of simulating a total of 12 different cases. These are outlined as follows:

Option 1: Reservoir storage routing to compute outflow hydrograph from reservoir with subcritical dynamic routing of outflow hydrograph through entire length of downstream valley--KUI=0, KKN=1, KSUPC=0, MULDAM=0.
Input data cards--1-4, 6-58.

Option 2: Reservoir storage routing to compute outflow hydrograph from reservoir with supercritical dynamic routing of outflow hydrograph through entire length of downstream valley--KUI=0, KKN=1, KSUPC=1, MULDAM=0.
Input data cards--1-4, 6-58.

Option 3: Reservoir storage routing to compute outflow hydrograph from reservoir with supercritical dynamic routing of outflow hydrograph through upstream portion of downstream valley and subcritical dynamic routing through downstream portion of downstream valley--KUI=0, KKN=2, KSUPC=1, MULDAM=0.
Input data cards--1-4, 6-52, 16-58.

Option 4: Same as Option 1 except reservoir dynamic routing to compute outflow hydrograph from reservoir--KUI=1, KKN=2, KSUPC=0, MULDAM=0.
Input data cards--1-4, 8-58, 63, 16-52.

Option 5: Same as Option 2 except reservoir dynamic routing to compute outflow hydrograph from reservoir--KUI=1, KKN=2, KSUPC=1, MULDAM=0.
Input data cards--1-4, 8-58, 63, 16-52

Option 6: Same as Option 3 except reservoir dynamic routing to compute outflow hydrograph from reservoir--KUI=1, KKN=3, KSUPC=1, MULDAM=0.
Input data cards--1-4, 8-58, 63, 16-52, 16-52.

Option 7: Subcritical dynamic routing of input hydrograph through a channel-valley--KUI=0, KKN=9, KSUPC=0, MULDAM=0.
Input data cards--1-4, 12-52. (See note on page A-20.)

Option 8: Supercritical dynamic routing of input hydrograph through a channel-valley--KUI=0, KKN=9, KSUPC=1, MULDAM=0.
Input data cards--1-4, 12-52. (See note on page A-20.

Option 9: "Sequential Method" Reservoir storage routing to compute outflow hydrograph from reservoir with subcritical dynamic routing of outflow hydrograph through downstream channel-reservoir having a dam which may fail--KUI=0, KKN=2, KSUPC=0, MULDAM=1.
Input data cards--1-4, 6-63, 16-63, ... 16-52.

Option 10: "Sequential Method" Reservoir dynamic routing to compute outflow hydrograph from reservoir with subcritical dynamic routing of outflow hydrograph through downstream channel-reservoir having a dam which may fail--KUI=1, KKN=3, KSUPC=0, MULDAM=1.
Input data cards--1-4, 8-58, 63, 16-63, ... 16-52.

Option 11: "Simultaneous Method" Simultaneous computation method for single dam or bridge (structure) using dynamic routing in the reach upstream of the structure and downstream of the structure with special internal boundary conditions for flow thru the structure--KUI=1, KKN=1, MULDAM=1, KSUPC=0.
Input data cards--1-5, 8-11, 12-58. See note on page A-21 for input variables for bridge and embankment.

Option 12: "Simultaneous Method" Simultaneous computation method for multiple dams and/or bridges (structures) using dynamic routing for all reaches with special internal boundary conditions for flow thru each structure--KUI=1, KKN=1, MULDAM=no. of dams and/or bridges, KSUPC=0.
Input data cards--1-5, 8-11, 8-11, 8-11, ... 12-58. See note on page A-21 for input variables and embankments.

"SIMULTANEOUS METHOD" OF COMPUTATION OF COMPLETE SYSTEM:

This option treats the upstream reservoir, any intermediate reservoir, and the downstream channel as one system. Cross sections are numbered consecutively from the very upstream end of the most upstream reservoir to the downstream extremity of the downstream channel. Cross sections are specified for the upstream and downstream sides of each dam. This option is most useful for problems in which the tailwater below a dam is affected by backwater from downstream dams or other constrictions. It is necessary when using this option to specify KKN=1, KUI=1, MULDAM $\geq$ 1 to read-in card (5). Also, cards (6) and (7) are omitted, and cards (8) and (9) are repeated for each dam in the system. Cards (59), (60), (61), (62), and (63) are not applicable for this option. MULDAM is defined as the number of dams in the system.

BRIDGE COMPUTATION

The simultaneous method can be used for either multiple dams or bridges. Cards (8) and (9) are used to describe the flow thru and across the bridge and embankment. The bridge embankment may be allowed to breach. If breaching is not considered possible, HF on card (9) is set to a very large value so that the water surface will not reach it. On card (8), RLM must be left blank as well as YO; other variables on card (8) are associated with the breach of the embankment and are defined essentially the same as shown on page A-4. The variables other than HF on card (9) are defined as follows: HD--height (ft m.s.l.) of crest of uppermost portion of road embankment; HSPD--length (ft) of crest of uppermost portion of road embankment measured across valley and perpendicular to flow; HGTD--height (ft m.s.l.) of crest of lower portion (emergency overflow) of road embankment (if non-existent, leave blank); CSD--length (ft) of crest of lower portion of road embankment measured across valley and perpendicular to flow; CGD--width of top of road embankment as measured parallel to flow; CDOD--coefficient of discharge of flow thru bridge opening (see: Chow, "Open-Channel Hydraulics" pp. 476-490); QT--time step to be used when the upper road embankment is overtopped. QT is only needed when the first structure in the routing reach is a bridge and when the inflow hydrograph is a slowly rising hydrograph. It should be left blank at all other times. If it is left blank when needed, the default value is 0.5 hr. Instead of reading in the length of the upper road embankment, a table of length of embankment (ft) vs. water surface elevation (ft msl) may be read in on cards (9) and (10) respectively. HSPD is then read in as zero.

ROUTING SPECIFIED INFLOW HYDROGRAPH (Options 7 and 8)

Options (7) and (8) are for routing a specified inflow hydrograph through the downstream valley, i.e., there is no upstream reservoir and associated outflow hydrograph as computed by DAMBRK. These options do not enable the treatment of bridges or dams located along the downstream valley.

LEVEL POOL ROUTING USING OPTIONS 11 AND 12

The storage routing (level pool) technique based on Eq. (18) may also be used simultaneously with the dynamic routing technique for simulating the unsteady flow through the downstream channel-valley. Eq. (18) is combined with Eq. (65) to form the upstream boundary condition and the dam is treated as an internal boundary via Eqs. (51-52). The advantages of this combination of the two routing techniques within a simultaneous computation method are: (1) simple routing technique for reservoir, (2) dynamic routing for downstream dam-break hydrograph, and (3) more accurate computation of tail-water elevation than via Eq. (11).

Level pool routing may be used with options 11 and 12 by: (1) including cards (6) and (7) after card (5); (2) IDAM(1) will always be 1, i.e., the first cross-section represents the upstream face of the first dam (level pool routing can only be used for the first or upstream reservoir).

FLOODPLAIN COMPARTMENTS (FPC)

Each FPC may have only one Δx-reach in which flow from the river enters the FPC or, if the differential head favors the FPC, the flow goes from the FPC to the river. This Δx-reach is designated by NXPI(K), where the K index goes from 1 to the total number of FPC's (KCG).

Each FPC may have only one Δx-reach in which the FPC pump(s) return water to the river. The Δx-reach is designated by NXPO(L), where the L index goes from 1 to the total number of pumps (NPM).

A particular Δx-reach cannot be used for more than one FPC; thus, NXPI(1)≠NXPI(2).

A particular Δx-reach cannot be used for both types of flow exchange (weir flow or pump flow); thus, NXPI(K)≠NXPO(L).

An FPC may pass flow to an adjacent FPC via broad-crested weir flow with submergence correction. Also, the most downstream FPC may pass flow on downstream via overtopping weir flow. FPC's are numbered from upstream to downstream, commencing on one side of the river and then the other side of the river.

TIME STEP SELECTION

The time step size used to route the hydrograph through the downstream channel-valley can be user controlled with the DTHM and TFI parameters on card (33). If a constant time step is desired, the user reads in DTHM (time step size) and leaves TFI blank.

If DTHM and TFI are both read in as zero, the model will generate an initial time step size based on the inflow hydrograph - TP/MDT where TP is the time from start of rise to peak of the hydrograph and MDT is the assumed to be 20 unless specified differently by reading in a negative DTHM value. This time step is used until time TFI (the time just prior to dam failure) is exceeded. If KUI=0 (card 2), this value is computed as the time to peak of the outflow hydrograph minus the time to failure. If KUI=1, TFI is set equal to TEH (card 12). If the time exceeds TFI or if the dam fails, the time step is cut back to TFH/MDT. If DTHM and TFI are read in as nonzero values, the DTHM is used until time TFI is exceeded and then the time step is cut back to TFH/MDT.

If TFI is read in as a nonzero value and DTHM is read in as zero, the model will compute DTHM=TP/MDT and use that time step until TFI is exceeded and then cut back to TFH/MDT.

UPDATE FEATURE:

If the parameters (BB, Z, TFH, HD, YO, HF) are the only ones that may have a different value than contained on all input data cards (1)-(63), the following UPDATE procedure can be used:

Place the following two cards immediately before card (1):

```
UPDATE  (with U starting in column 1)
BB, Z, TFH, HD, YO, HF -- 6F10.0
```

where BB, Z, etc., are defined as described previously on cards (8)-(9). If any of these values do not change, leave the appropriate space blank. The update feature is only applicable for Options 1-6.